(2)

NAVAL POSTGRADUATE SCHOOL
Monterey, California

THESIS

EFFECTS OF NEUTRON IRRADIATION ON
HIGH TEMPERATURE SUPERCONDUCTORS

by

John J. Hammerer, Jr.

June 1988

Thesis Advisor F.R. Buskirk

Unclassified

security classification of this page

REPORT DOCUMENTATION PAGE

1a Report Security Classification: Unclassified			1b Restrictive Markings
2a Security Classification Authority			3 Distribution Availability of Report: Approved for public release; distribution is unlimited.
2b Declassification Downgrading Schedule			
4 Performing Organization Report Number(s)			5 Monitoring Organization Report Number(s)
6a Name of Performing Organization: Naval Postgraduate School	6b Office Symbol (if applicable): 33		7a Name of Monitoring Organization: Naval Postgraduate School
6c Address (city, state, and ZIP code): Monterey, CA 93943-5000			7b Address (city, state, and ZIP code): Monterey, CA 93943-5000
8a Name of Funding Sponsoring Organization	8b Office Symbol (if applicable)		9 Procurement Instrument Identification Number
8c Address (city, state, and ZIP code)			10 Source of Funding Numbers
		Program Element No	Project No / Task No / Work Unit Accession No

11 Title (Include security classification): EFFECTS OF NEUTRON IRRADIATION ON HIGH TEMPERATURE SUPER-CONDUCTORS

12 Personal Author(s): John J. Hammerer, Jr.

13a Type of Report	13b Time Covered	14 Date of Report (year, month, day)	15 Page Count
Master's Thesis	From To	June 1988	60

16 Supplementary Notation: The views expressed in this thesis are those of the author and do not reflect the official policy or position of the Department of Defense or the U.S. Government.

17 Cosati Codes			18 Subject Terms (continue on reverse if necessary and identify by block number)
Field	Group	Subgroup	radiation effects; high temperature superconductivity,

19 Abstract (continue on reverse if necessary and identify by block number)

Neutron irradiation of high temperature superconductors was performed in order to determine the effects of nuclear weapons on these novel materials. This radiation could also be encountered in space radiation belts, fusion reactors and particle accelerators. Fluences used were on the order of 10^{18} fast and thermal neutrons cm^2. The result of the irradiation was a complete loss of observed superconductivity in $YBa_2Cu_3O_7$ and $ErBa_2Cu_3O_7$. A combination of gamma heating of 5 W/g and fast neutron flux imposed severe thermal stress on sample pellets. In two cases, the pellets were reduced to powder. Samples were prepared at the Naval Research Laboratory and the National Bureau of Standards. They were checked for the Meissner effect using magnetic levitation. The dc four terminal method was used to determine the transition temperature. Irradiation of samples was conducted in the Omega West Nuclear Reactor at the Los Alamos National Laboratory.

20 Distribution Availability of Abstract	21 Abstract Security Classification	
☒ unclassified unlimited ☐ same as report ☐ DTIC users	Unclassified	
22a Name of Responsible Individual: F.R. Buskirk	22b Telephone (include Area code): (408) 646-2765	22c Office Symbol: 61Bs

DD FORM 1473,84 MAR — 83 APR edition may be used until exhausted. All other editions are obsolete.

security classification of this page

Unclassified

Approved for public release; distribution is unlimited.

Effects of Neutron Irradiation on
High Temperature Superconductors

by

John J. Hammerer, Jr.
Lieutenant Commander, United States Navy
B.S., University of South Carolina, 1976

Submitted in partial fulfillment of the
requirements for the degree of

MASTER OF SCIENCE IN PHYSICS

from the

NAVAL POSTGRADUATE SCHOOL
June 1988

Author: John J. Hammerer, Jr.
John J. Hammerer, Jr.

Approved by: Fred R Buskirk
F.R. Buskirk, Thesis Advisor

Karen K. Maruyama
X.K. Maruyama, Second Reader

K.E. Woehler
K.E. Woehler, Chairman,
Department of Physics

G.E. Schacher
Gordon E. Schacher,
Dean of Science and Engineering

ABSTRACT

Neutron irradiation of high temperature superconductors was performed in order to determine the effects of nuclear weapons on these novel materials. This radiation could also be encountered in space radiation belts, fusion reactors and particle accelerators. Fluences used were on the order of 10^{18} fast and thermal neutrons/cm^2. The result of the irradiation was a complete loss of observed superconductivity in $YBa_2Cu_3O_7$ and $ErBa_2Cu_3O_7$. A combination of gamma heating of 5 W/g and fast neutron flux imposed severe thermal stress on sample pellets. In two cases, the pellets were reduced to powder. Samples were prepared at the Naval Research Laboratory and the National Bureau of Standards. They were checked for the Meissner effect using magnetic levitation. The dc four terminal method was used to determine the transition temperature. Irradiation of samples was conducted in the Omega West Nuclear Reactor at the Los Alamos National Laboratory.

TABLE OF CONTENTS

LIST OF TABLES

LIST OF FIGURES

ACKNOWLEDGMENTS

In an academic pursuit such as this, the novice author relies on the advice and counsel of many in order to achieve a successful result. I am grateful to Professors Fred Buskirk and Xavier Maruyama of the Naval Postgraduate School. They are responsible for kindling in me a newfound respect for and enjoyment of experimental physics.

I also thank Dr. S. A. Wolf and his outstanding staff at the Naval Research Laboratory for their material support and sharing their long recognized and widely respected expertise in the field of superconductivity. Dr. M. S. Osofsky was especially helpful in explaining the subtleties of experimental procedures involved in this project.

I am thankful to Dr. D. Ederer of the National Bureau of Standards for providing test samples and Dr. M. Bunker of Los Alamos National Laboratory for assisting in the irradiations.

I am particularly appreciative of the assistance rendered by Dr. T. Hofler and Mr. G. Pless of the Naval Postgraduate School. Their help with the thermometry and electronic equipment aspects of the experiment was invaluable.

I acknowledge, with pleasure, the contributions of [redacted] to the construction of the vacuum system used in the experiment.

Finally, in the spirit of saving the best for last, I am indebted to [redacted] Without her constant support, understanding and encouragement, the successful completion of this work would not have been possible.

I. INTRODUCTION

A. OVERVIEW

Since the discovery of high temperature superconductors (HTS) in 1986 by Nobel Laureates J. G. Bednorz and K. A. Muller, exhaustive research has been conducted worldwide to characterize the novel material which promises to revolutionize current electrical and electronic technology. While the promises of low temperature superconductivity were great, naval applications have been few. The benefits afforded by the superconductivity were literally outweighed by the auxiliary equipment needed to maintain temperatures below 30 K. The advent of HTS which operate in the easily and inexpensively attained liquid nitrogen temperature regime have renewed the promise for naval applications. Careful consideration of the possible combat environments in which these materials will be expected to operate indicates that nuclear effects on HTS must be explored.

B. PURPOSE OF EXPERIMENT

This experiment sought to determine the effects of neutron irradiation of high temperature superconductors. Specifically, this experiment investigates the effects of thermal and fast neutron fluence on the order of 10^{18} neutrons/cm^2 on the transition temperature (T_c) of yttrium and erbium superconductors. The flux consisted of slow and fast neutrons produced in the core of the Omega West Reactor. This flux is described in more detail in section III B. A significant amount of research and development in the area of superconducting thin films has already been conducted. Most likely, one of the first applications of HTS wil be in the advanced technology required for the Strategic Defense Initiative. In the combat environment of space, HTS could be subjected to high neutron fluxes as the result of nuclear explosions. Thus, with early deployment of the system a possibility, it has become imperative to learn as much as possible about the behavior of these materials in the nuclear environment. While this research is basic in nature, the results it yields should be of considerable value to those concerned with emerging practical applications.

C. HISTORY OF SUPERCONDUCTIVITY

The phenomenon of superconductivity in mercury was discovered in 1911 by Heike Kamerlingh Onnes shortly after he was able to achieve temperatures below 4 K with

liquid helium. The prospect of materials without electrical resistance created great interest in the scientific world. Experimentalists began in earnest to look for other materials whose electrical resistance vanished at higher temperatures. Unfortunately, their efforts were rewarded with only minor advances. By 1941 Aschermanner, Friederich, Justi and Kramer reported superconductivity in NbN near 16 K. In 1954, Hardy and Hulm had succeeded in raising the barrier to 23 K using cubic A15 structure type materials. In the 1960's the search was expanded to include organic, layered and oxide compounds. However, given the success of the Niobium A15 cubic materials , most researchers tended to concentrate on that aspect. In 1972 superconductivity was discovered in $PbMO_6S_8$, a ternary superconductor. Many reports of high transition temperatures in compounds such as CuCl (140 K), CdS (150 K), bile cholates (140 K) and dilute alkali solutions of ammonia (180 K) contained results which could not be reproduced. Superconductivity was confirmed in p-type GeTe in 1964 by Hein and in $SrTiO_3$ by Schooley et al. in 1965 but these had transition temperatures less than 1 K. In 1973, Johnston discovered superconductivity in $LiTiO_3$ at 13 K and in 1975 superconductivity was confirmed in $PbBiBaO_3$ at 14 K. These last two discoveries are particularly important in the history of HTS because these materials are oxide perovskites characteristic of current HTS. [Ref. 1: p. 1]

The advance of greatest practical importance prior to that of Bednorz and Muller was made by Kunzler. In 1961, he discovered high field, high current superconductors. This meant that the high current densities and high fields necessary for practical applications could be achieved without the catastrophic failure previously encountered in low field superconductors. [Ref. 2: p. 17]

Perhaps even more difficult than the search for high temperature superconductors has been the effort to understand the physical principles of superconductivity. Originally it was thought that the phenomenon was simply the loss of resistance. In 1924 W. H. Keeson applied thermodynamic principles to explain the transition to superconductivity. A phenomenological explanation of the second order transition was advanced by Gorter and Casimir in 1934 based on a two fluid model. In 1935 the London brothers employed a combination of Maxwell's equations and two assumptions to account for the Meissner effect and infinite conductivity. They postulated that the curl of the supercurrent, J_s, was proportional to the negative of the magnetic field and assumed that the time derivative of the supercurrent was proportional to the electric field [Ref. 3: p. 327]. Although their theory was successful in explaining the Meissner effect and infinite conductivity, a

detailed comparison with experimental results showed several serious descrepancies. Nonetheless, their work provided foundations for Peppard, Ginzberg and Landau [Ref. 4: p. 37]. A significant contribution was made to the theory in 1950 when H. Frohlich developed a theory based on the interaction of electrons with vibrating atoms in the crystal lattice which explains the isotope effect, but failed to predict the other properties of the superconducting state [Ref. 3: p. 320]. The prediction that superconductors could be classified as Type I (low field) or Type II (high field) came as the result of the work of Ginzberg, Landau, Abrikosov and Gorkov (GLAG) in 1950 [Ref. 2: p .17].

Cooper observed in 1956 that if one considered two electrons slightly excited from the Fermi sea they could form a real bound state provided there was a weak attractive potential [Ref. 5: p. 45] By far the most comprehensive and successful explanation to date was developed by Nobel Laureates J. Bardeen, L. Cooper and J. Schrieffer. Their quantum mechanical theory successfully accounts for the Meissner effect and other thermodynamic and electromagnetic properties of superconductors.

The now well known work of Bednorz, Muller and Chu catapulted high temperature superconductivity into the limelight of public as well as scientific attention. At this writing the highest reproducible transition temperature achieved is 125 K in a system of Tl-Ca-Ba-Cu-O by the IBM Almaden group [Ref. 6: p. 21].

D. APPLICATIONS

The applications of superconductivity have lagged even further behind experimental and theoretical work. Most of the applications have been restricted to the laboratory, in particular , electromagnets for accelerators and plasma devices. The most well known exception is magnetic resonance imaging systems which require large magnetic fields for medical diagnosis. The most recently publicized use was for levitation and propulsion of high speed trains in Japan. A currently much debated application is the superconducting supercollider accelerator for elementary particle research. Much of the knowledge generated in the field of superconductivity is a direct result of the extensive work done on magnetic confinement systems for nuclear fusion reactors. Naval applications have included communications antennae developed by the Naval Research Laboratory and superconducting electric power generation and propulsion systems designed, built and tested by the David Taylor Naval Ship Research and Development Center [Ref. 7].

The most immediate application of HTS will most likely be in thin film technology. The difficulty in fabricating large HTS components is due to the inherent brittleness of the ceramic material and possible problems of stability.

II. THEORY

A. PHYSICAL PHENOMENON OF SUPERCONDUCTIVITY

Although the theory of superconductivity is extremely sophisticated and strongly reliant on quantum mechanics, the basic properties of superconductors are easily comprehended. The two readily observable characteristics of superconductors are that they have infinite conductivity (or equivalently, zero electrical resistance to current flow) and they expel magnetic fields from their bulk (Meissner Effect) . Superconductors can be classified according to the temperature at which they transition to the superconducting state. Those with transtion temperatures (T_c) below 20 K are known as low temperature superconductors and above 20 K as high temperature superconductors. Superconductors can be further divided on the basis of their response in magnetic fields. Type I superconductors are distinguished by the fact that magnetic fields less than a certain critical field H_c are excluded from the material and current flow meets no resistance. Fields greater than H_c cause simultaneous penetration of the field into the interior of the material and resistance proportional to the electric field and applied current is restored. The value of H_c is typically on the order of one T. Type II superconductors experience magnetic field penetration at one value H_{c1} , but continue to exhibit zero resistance to current flow up to a higher value of the applied magnetic field H_{c2} on the order of 40 T and greater and capable of supporting current densities of 10^5 A / cm^2. [Ref. 8: p. 470]

It should be noted:

> ...that when the current through a superconductor alternates, small absorptions of energy roughly proportional to the rate of alternation occur. When the frequency of alternation rises above 10 MHz appreciable resistance arises and at infrared(10^{13} Hz) the resistivity is the same as the normal and superconducting states and independent of temperature. [Ref. 2: p. 1]

The classical explanation of current flow through a conductor is based of the idea that mobile valence electrons flow through the crystal lattice of the material accelerated by an electric field. Their motion is impeded by lattice impurities, geometric imperfections (such as grain boundries) and thermally induced imperfections [Ref. 3: p. 153]. Thus, it is not difficult to understand why Kamerlingh Onnes found superconductivity in highly purified mercury (melting point 234 K) at 4.2 K. The re-

sistance to current flow as a characteristic property of any material is expressed in terms of the resistivity of the material and is given by:

$$\rho = \frac{VA}{Il}, \tag{1}$$

where V is the voltage drop across the sample, I is the current through the sample, A is the sample's cross sectional area and l its length. Typical values of resistivity range from 1.6 x 10^{-8} Ω -m for silver to 9 x 10^{11} Ω -m for glass. The temperature coefficient of resistivity describes the fraction change in resistivity per degree C with the value for silver being 3.8 x 10^{-3}/° C. [Ref. 9: p. 699]. From equation 1 it can be seen that V/I = R. Thus, for the superconducting state with R equal to zero, ρ must be zero.

B. MECHANISMS OF SUPERCONDUCTIVITY

The culmination of the advancement from the classical theory to the quantum theory of superconductivity is the BCS theory. It successfully accounts for:

- Effects associated with infinite conductivity ($\vec{E} = 0$)
- The Meissner Effect ($\vec{B} = 0$)
- The dependence of T_c on isotopic mass and $T_c \sqrt{M}$ = constant
- Second order phase transition at T_c
- Electronic specific heat varying as $\exp(-T_0/T)$ near T = 0 and other evidence for an energy gap for individual particle-like excitations. [Ref. 10]

BCS theory built on a number of concepts previously proposed which only partially accounted for all of these phenomomena. Gorter and Casimir's two fluid model proposed that two types of electrons, superconducting and conventional, existed in superconducting material. When superconductivity was attained, the superconducting electrons played the dominant role. H. London and F. London suggested the possibility of an energy band gap between the electronic states in superconducting material and long range order in momentum space. H. Frohlich theorized that an interaction between electrons and phonons was the mechanism responsible for the superconductivity. [Ref. 4: p. 46]

Cooper pointed out that if there were a net attractive force between pairs of electrons it would be possible to achieve the more stable low energy superconducting electronic state [Ref. 11: p. 103]. This could be achieved by an electron interacting with ions in the crystal lattice. The electron - ion attraction transfers momentum to the ion

which then propagates the additional momentum through the lattice as a thermal vibrational wave (phonon). If at some distance away from the original electron ion interaction a second attractive phonon - electron interaction occurs, momentum will have been transferred from one electron to another through an attractive process. Through the medium of phonon momentum transfer, an attractive force has been established between two electrons over a relatively long distance. More correctly, the lattice vibrations are of such short duration according to the uncertainty principle, they don't last long enough to be observed before being absorbed [Ref. 11: p. 103]. This attractive situation is energetically more favorable for the electrons. Hence, in the ground state the density of these pairs of attractive electrons (Cooper pairs) is increased dramatically. When an overwhelming majority of the electrons in the lattice exist in the Cooper pair configuration, momentum can be transferred in a highly synchronized, uniform fashion without the random scattering of electrons from lattice imperfections typical of resisted current flow.

Indeed, the discovery by Daunt and Mendelssohn in 1946 that there was no Joule heat in the superconducting state confirmed the lack of entropy in the supercurrent, proving conclusively the existence of the energy gap [Ref. 11: p. 106]. When the electrons are in the highly ordered ground state and an electric field is applied, all of the Cooper pairs move through the lattice with exactly the same momentum. The motion of each Cooper pair is synchronized with all other pairs thus the random motion responsible for resistance is avoided [Ref. 12: p. 488]. In regard to the Meissner effect, it is important to note that according to electromagnetic theory there must be a transition zone between a region of finite magnetic field and zero magnetic field. The London equation and BCS theory make it possible to determine the penetration depth of the field into the superconductor. The degree of penetration is dependent upon sample geometry and temperature [Ref. 2: p. 7-8]. GLAG theory successfully explains the behavior of Type I and Type II superconductors in terms of surface energy of the normal - superconductor interface. At the root of the theory is a factor, κ , related to the surface energy. Type I superconductors have positive surface energy and $\kappa < 1/\sqrt{2}$ and Type II superconductors have negative surface energy with $\kappa > 1/\sqrt{2}$ [Ref. 2: p. 17]. GLAG theory reduces to London theory as κ approaches zero [Ref. 4: p. 45].

Recent work aimed at confirming the applicablity of BCS theory to the behavior of HTS has had mixed results. Walter et al. examined characteristics of the energy gap in La-Sr-Cu-O HTS using far infrared techniques and found that while an energy gap ex-

isted, its magnitude was not as predicted by BCS strong or weak coupling. This suggested that a novel mechanism was required [Ref. 13]. The isotope effect in Y-Ba-Cu-O and Ba-Eu-Cu-O HTS was studied by Batlogg et al. [Ref. 14] and Bourne et al. [Ref. 15]. Both experiments found no or insignificant differences in T_c for compounds with O^{18} substituted for O^{16}. Again, while the BCS phonon - electron exchange mechanism may be valid for some phenomena of HTS, it appears that it does not fully explain the isotope effect or the energy gap. On the positive side, Weber [Ref.16] noted that high T_c values for La-(Sr,Ba)-Cu-O HTS were caused by very large electron - phonon coupling and that it is mainly caused by the oxygen p orbital of the conduction band involving specific oxygen vibrations and the light oxygen mass is instrumental for reaching the high T_c values. Other possibilities still being considered include plasmons, charge transfer excitations, spin fluctuations or resonating valence bond interactions [Ref. 17].

The uncertainty in the theory of the mechanism of HTS is not limited to momentum transfer interactions. The path of electron flow in the lattice is also controversial at this writing. Most evidence seems to indicate that the presence or absence of oxygen atoms plays a critical role. In the perovskite structure, oxygen vacancies serve to electrically isolate the rare earth planes from the copper planes . In the copper planes, oxygen vacancies are responsible for the chain-like formations which carry the current [Ref. 18: p. 248).

Much evidence exists to support the theory that the orthorhombic oxygen deficient perovskite lattice is responsible for superconductivity in $YBa_2Cu_3O_{7-x}$. Toth et al. found that samples with tetragonal structure exhibited broadened transitions, and incomplete flux explusion while the orthorhombic HTS had sharp transitions and nearly complete flux expulsion. They correlated superconductivity with the ordering of oxygen atoms on the basal plane producing one dimensional Cu-O chains [Ref. 19: p. 44]. Similiar results were obtained by Golben et al. for Er-Ba-Cu-O . They concluded that it also is an orthorhombic perovskite structure with the Er atom sandwiched between the Ba atoms [Ref. 20].

Pauling believes that the CuO_4 squares have infinite straight lines of alternating Cu and O atoms in the a and b crystallographic directions and that this structure, interacting with layers of La and other metals gives rise to superconductivity [Ref. 21]. Teller suggests that vibrations of oxygen atoms at frequencies characteristic of ultraviolet light make the Cooper pairs [Ref. 22: p. 358]

Oxygen atom positions and oxygen site occupancies in the lattice have been verified by neutron powder diffraction methods. These experiments have revealed that oxygen vacancy ordering in the Cu-O basal plane of the Y-Ba-Cu-O system plays a key role in the tetragonal to octahedral phase transition. Neutron powder diffraction methods have resulted in the following observations:

- the orthorhombic to tetragonal phase transition is driven by the disordering of oxygen atoms in the Cu-O basal plane
- the transition temperature occurs at an oxygen stoichiometry of approximately 6.5
- the phase transition is continuous driven by disorder of Cu-O planes

Sanchez et al . have proposed a thermodynamic model based on interactions of O-O nearest neighbors. They investigated the finite temperature behavior of oxygen using the configuration entropy calculated in the square approximation of the cluster variation method. They speculate that structural changes produced by rare earth substitutions decrease O-O repulsion which decreases the ordering on the basal plane thus lowering the transition temperature. Even if O-O repulsion itself is not responsible for the decrease in T_c for La HTS and lack of superconductivity in Pr-Ba-Cu-O, the increase in the lattice constant results in a lower degree of basal plane ordering. Finally, they note that the increase in O-O repulsion should increase the degree of ordering on the basal plane which may result in higher superconducting temperatures. [Ref. 23]

Only minor exceptions to the overwhelming evidence of the correlation between ordered Cu-O planes and superconductivity have been noted in the literature. Gallagher and Dinger of IBM measured the coherence lengths in single crystals of $YBa_2Cu_3O_x$ in directions parallel, perpendicular and at several angles in between the Cu-O chains. The coherence length is the length over which the quantum mechanical wave functions of the superconducting electrons extend. They found that no significant difference in the measurements in any direction. In fact, their results indicated that the flow of the supercurrent may be three dimensional. Had the linear Cu-O chains been responsible for HTS, some significant difference in the coherence length should have been detected. Maeno, of Hiroshima University, substituted iron and other elements for Y. He found that at two percent substitution, despite the transition to tetragonal structure, superconductivity was still present. This also suggested that long chains may not be necessary for superconductivity above 90 K. [Ref. 18: p. 249]

In summary, the majority of work completed to date indicates that HTS known at the present time are associated with oxygen deficient perovskite structures. The

orthorhombic phase is superconducting while the tetragonal phase is not. Further, in the orthorhombic phase, the highly ordered Cu-O basal plane is the current flow path in the superconducting state and Cu-O chains within that plane are seen many as the primary flow path for the supercurrent. These findings are supported by experimental results such as effects of oxygen stoichiometry on T_c and neutron powder diffraction. Theoretical calculations for the effects of varying the amount of oxygen in the basal plane agree with the experimental results.

C. RADIATION DAMAGE MECHANISMS

The theory and experimental results of radiation damage studies are well known and understood for many materials.A brief review of the principles involved will make interpretation of the experimental observations more meaningful.

Crystalline materials such as HTS are formed in a regular lattice arrangement. The critical importance of the ordered structure and stoichiometry to HTS has been discussed in detail. Neutron induced defects in the lattice could therefore have an effect on superconducting properties.

Neutrons are most commonly classified according to their energy. Slow or thermal neutrons are those with energies less then about 100 eV. At room temperature, the most probable energy is about 0.025 eV. Fast neutrons are those with energies greater than 10 keV. A further division corresponds to neutrons with energies greater than 0.4 eV. These are known as epicadmium neutrons. Cadmium can be used to absorb neutrons with energies below approximately 0.4 eV. At energies above this the capture cross section for cadmium becomes negligible. [Ref. 24: p. 22]

Neutrons interact with lattice atoms by either of two processes, absorption or scattering. In the absorption reaction, a neutron is absorbed by the nucleus. This results in a new species which may be radioactively stable or unstable. The probability for absorption is greater for neutrons of lower energy and atoms of greater mass. Scattering reactions can be further classified as elastic or inelastic. Elastic collisions are those involving low energy neutrons which do not leave the target nucleus in an excited state, while inelastic collisions leave the target nucleus in an excited state as well as transferring kinetic energy. Fast neutrons are required for the inelastic reaction in order to provide energy sufficient to raise the nucleus to the next higher quantum state. A generally accepted value of the energy required to displace an atom from its lattice site is 25 eV. Thus, only fast neutrons have enough energy to displace atoms from their positions in the lattice.

Difficulties with respect to fast neutrons are that the reactor supplies fast neutrons with a spectrum of energies and measurement of the spectrum is neither easy nor accurate. Reactor fast neutrons are contaminated by gamma rays and thermal neutrons that respectively cause ionization damage (heating) and activation of specimens. In experimental reactors,the fast neutrons can be found in quantity only in the core and gradients in the fast neutron flux will be steep. All of these factors contribute to experimental difficulties. [Ref. 25: p. 54]

The probability that a nucleus will participate in a scattering or absorption reaction with a neutron is also energy dependent and expressed in terms of the scattering or absorption cross section in barns (10^{-24} cm^2). Generally speaking, the higher the energy of the incident neutron, the lower the cross section for scattering or absorption [Ref. 26: p. 362].

Also significant in neutron - nucleus interactions is the fact that there is no coulomb force between the two. This means that more of the initial kinetic energy of the incident particle is available for transfer to target nuclei in the lattice [Ref. 27: p. 277].

Once the neutron - nucleus interaction occurs, several types of defects can be produced in the lattice. They include:

- Vacancies - Incident neutrons displace atoms from their lattice sites. Displaced atoms can possess large amounts of kinetic energy which they transfer by secondary collisions with other atoms in the lattice . This is known as the cascade effect and accounts for much more damage than the initial neutron collision.
- Interstitials - When a displaced atom comes to rest in the crystal at a position other than an established lattice site it is known as an interstitial vacancy. These present a major obstacle to the propagation of phonons. Any HTS which relies on phonon interactions as a mechanism for supercurrent flow will have degraded performance due to interstitial defects.
- Frenkel defects - These are vacancy -interstitial pairs in the lattice.
- Impurities - Some of the atoms in the lattice may have absorption cross sections sufficiently large to permit a great percentage of incident neutrons to cause transmutations of lattice atoms. These defects could be manifested as isotopic effects or distortion of the lattice to such an extent that superconductivity could be destroyed.
- Thermal spikes - Rapid heating and quenching of a small volume of material can occur in the immediate vicinity of primary and secondary collision points. In the collision process the kinetic energy of the incident particle is converted to translational and vibrational energy of the lattice atoms producing sufficient local heating to cause melting [Ref. 27: p. 135]. This becomes an important factor to consider since the rapid quenching can cause formation of the non-superconducting tetragonal phase.
- Dimensional changes - occur in the anisotropic lattices of materials subjected to fast particle irradiation. Graphite and uranium are the best known examples. Some directions in the lattice may increase while others simultaneously decrease.

This occurs due to preferential energy levels associated with sites for interstitials. [Ref. 25: p. 26]

In considering the applicability of the final defect to irradiation of HTS, due consideration should be given to the work of Veronin et al., They exposed HTS samples to neutron (E > 1.0 MeV) fluences from 5 x 10^{17} to 1 x 10^{19} neutrons/cm^2. Using neutron diffraction techniques, they found that none of the samples underwent any phase change even though T_c had been lowered by many tens of degrees. [Ref. 28]

Materials irradiated in nuclear reactors can also be subjected to the effects of gamma radiation. The photoelectric effect, Compton scattering and pair production can produce electrons which can cause displacements. In fast and thermal neutron experiments, the gamma flux is usually unimportant unless it is high enough to cause undesirable gamma heating or thermal stress from gamma heating [Ref. 25: p. 89]. Ceramic materials, which include HTS, become appreciably altered at thermal neutron fluences greater than 10^{19} neutrons cm^2 .[Ref. 25: p. 214]

One further aspect of radiation damage is that it is sometimes reversible through the annealing process. Once displacement defects are created, sufficient energy remains in the lattice to permit continued mobility of vacancies and interstices. When a vacancy and interstitial combine, the defect is eliminated. Annealing in metals can take place at low temperatures. Annealing peaks in copper have been observed at 17 K [Ref. 24: p. 41]. However for neutron induced effects in semiconductors, temperatures in excess of 420 K are required. A very slow annealing is experienced when irradiated semiconductor devices are permitted to rest for several months at room temperature [Ref. 24: p. 61].

In light of the effects of neutron irradiation on crystal structure, it appears that HTS which rely on a high degree of order in the lattice, precise stoichiometry and phonon interaction for supercurrent flow will be susceptible to radiation damage.

III. EXPERIMENTAL PROCEDURE

Determining the effects of neutron radiation on the transition temperatures of HTS is relatively straightforward. Samples of material were provided by the ceramics group at the Naval Research Laboratory (NRL) and by D. Ederer of the National Bureau of Standards (NBS). The steps involved included verification of superconductivity prior to irradiation, initial measurement of resistivity, irradiation, and a post irradiation comparative measurement of resistivity to determine the radiation effects.The dc four terminal method was used for resistivity measurements.

A. SAMPLE PREPARATION

The preparation of HTS material is based on the calcining and sintering of constituent oxide powders. While preparation does not require techonologically sophisticated equipment, the quality of the material is highly process dependent.

The methods used at the Naval Research Laboratory ceramics laboratory to prepare the Erbium based superconductors are typical of the techniques used in preparing HTS. The stoichiometrically correct amounts of 99.999% pure powders of erbium oxide (Er_2O_3), barium carbonate (Ba_2O_3), and copper oxide (CuO) were weighed out on a precision balance. Care was taken to avoid any inhalation or absorption of the barium compound as it is toxic in small amounts [Ref. 29: p.185]. The powders were mixed with mortar and pestle then transferred to a clean ceramic container and mounted in a "spex mill" (a standard laboratory mixing machine, in design, not unlike commercial paint mixing machines) for ten minutes of mixing. The purpose of thorough mixing is to produce powders with grain size of the order of ten microns [Ref. 30]. This provides greater surface area for the reaction to occur. The mixed powder was placed in a platinum foil crucible and placed in a room temperature furnace. The furnace temperature was increased at a rate of 10 K/minute up to a temperature of 1210 K. The powder was calcined for four hours at this temperature. Calcining decomposes the barium carbonate to an oxide with carbon dioxide as a by-product. One problem in calcining is that the carbonates remain stable and do not always decompose. Furthermore, at the reaction temperatures, particle sintering and grain growth occur. Thus, the calcined materials must be remilled [Ref. 30]. After calcining, the powder was withdrawn from the furnace and quickly reground by mortar and pestle and milling to obtain an even consistancy. The powder was then cold pressed into disc shaped pellets using a pressure

of 1.38 kbar. The dimensions of the NRL pellets were typically 1.3 cm in diameter and 0.5 cm high. The pellets were returned in a platinum crucible to a tube furnace with flowing oxygen at atmospheric pressure. The temperature was increased at a rate of 1 K minute to 573 K, then at 5 K minute to 1210 K. Samples were held at 1210 K for four hours then cooled to 623 K at a rate of 1 K minute before being removed to room temperature. The sintering and slow cooling process is critical to the formation of HTS. Too much or too little oxygen in the material can cause severe degradation of superconducting properties. Whenever possible, the samples were kept in dessicators to prevent absorption of water vapor from the air.

B. EQUIPMENT CONFIGURATION

The two principle requirements for conducting the four terminal resistivity measurement of the sample were suitable electronic equipment and a cryogenic environment. The four terminal method requires a current source and a nanovoltmeter. Originally it was thought that the four wire ohm measurement function of the HP 3456A digital voltmeter would be suitable for the experiment. The accuracy of the HP 3456A voltmeter is 0.0024 percent in the 0.1 volt range. Unfortunately, the current supplied by the instrument in the built-in four wire ohms function is restricted to 1.0 mA output current in the 100 ohm range in which most of the samples fell. Because a greater input current was required, a simple HP 6218A power supply was used in series with a 900 ohm resistor to provide the current source. The dc voltage function of the HP 3456A was used with the math function to produce an output signal in milliamps. Before actually testing samples, the equipment mentioned above was interfaced with the computer, the control program written and simulated measurements conducted using the power supply to mimic the test signal. Figure 1 is a block diagram of the measurement system. [Ref. 31: p. 1-2]

One of the most attractive features of HTS is that they transition to the superconducting regime at or above the temperature of liquid nitrogen. In order to determine the transition temperature a cryogenic environment for the sample was devised. A cylindrical dewar 30 cm long and 3.7 cm in diameter was filled to a depth of 4 cm with liquid nitrogen. A cryogenic mounting stand (CMS) (Figure 2) was machined from copper. Copper was selected for its superior thermal conductivity . The 5 cm diameter, 0.5 cm thick base of the CMS was immersed in the liquid nitrogen. Atop the 8.5 cm pedestal was the disc-shaped sample holder which typically was 2.5 cm above the nitrogen level. the sample holder had a machined 0.6 cm circular depression filled with thermally

conductive, electrically insulating grease. This thermally coupled the sample to the CMS to promote heat flow , electrically isolated it from the CMS and served to mechanically stablize the sample while inserting it into the dewar. A 0.3 cm passage was drilled into the sample holder to enable a chromel-constantan thermocouple to be imbedded in the thermoconductive paste. Two threaded brass guide posts were attached to the sample holder to neatly guide the leads out through the dewar top and to act as an extension of the heat sink. This was so that the wires could be wrapped around the posts to avoid temperature gradients and resultant thermal emf.

The samples tested transitioned at temperatures of approximately 93 K but did not reach the superconducting state fully until 80 K. In order to achieve temperatures of approximately 70 K a vacuum was raised above the nitrogen. This was done by connecting the dewar to the house vacuum system via 1 mm plastic tubing to a glass tee in the cork stopper. The third point of the tee was connected to a standard vacuum gage. The top of the dewar was sealed with modeling compound. This arrangement made it possible to achieve nominal temperatures of 70 K at a vacuum of 300 mm Hg.

In a sensitive measurement such as this one the selection of wire for the four terminal leads is of no small significance. A compromise on properties had to be made. Originally manganin wire was selected because of its low thermal conductivity . This feature was attractive because it minimized the thermal energy flow to the sample. Unfortunately, the resistance of manganin wire was in excess of the digital voltmeter manufacturer's specifications for four wire ohm measurements which was 10 ohms. Therefore, lower resistance copper wire was used. To minimize the problem of heat flow and thermal emf in these wires they were wrapped around the CMS guide posts to reduce the thermal gradient. Later the wires were taped to the side of the sample holder. Lacquer insulation was stripped from both ends of the wire using a hot wire stripper and emery cloth. In order to make better electrical and mechanical contact a small 1.0 mm diameter loop was formed at the sample end of the wire before it was attached to the sample.

Many different methods exist for attaching the wires to the sample. They include screw contact points, pressure contact points, standard and ultrasonic soldering techniques and electric conductive compound (ECC) such as the material with the tradename "Nickleprint". Attempts were made to attach the leads with 99.99% indium using standard soldering techniques but contact was difficult to maintain. The ECC technique was used throughout the experiment with good success. The technique which

proved most successful for applying the ECC was to dip a 1 cm long 0.2 mm diameter wire held by tweezers into the ECC extracting a few small drops. With the copper lead firmly in contact with the pellet, the ECC was dropped onto the lead and allowed to dry for several minutes. Two different geometries for contact points were used. The first was a linear, across the diameter of the flat surface. The second arrangement was square with contact points at the corners of the square.

The primary means of determining the temperature of the transition was with a chromel-constantan thermocouple. The manufacturer's limit of error for this type E thermocouple in the range 73 K to 273 K is 1.7 K or one percent, whichever is greater. The thermocouple was fabricated by soldering teflon coated 0.25 mm chromel and constantan wire together. The thermocouple was imbedded the thermal compound and the leads connected to an Omega Omni Amp IIB thermocouple dc millivolt amplifier with cold junction compensation. The assumption was made that because the thermocouple, thermal compound and sample were in such close physical proximity, the system was in equilibrium. The amplifier output was them sent to an HP 3478A multimeter for readout and transmission via an HP-IB interface bus to the HP 86B computer. The millvolt reading (v) was converted to Kelvin temperature using a fourth order polynomial:

$$T = 1.58630 + 16.9113v - .262371v^2 + .06729v^3 + .0138366v^4 + .00126431v^5 \quad (1)$$

This equation was derived from the NBS thermocouple tables using a curve fitting program based on the least squares fit method [Ref. 32: p. T-44]. The thermocouple was calibrated a minimum of twice a day. It was compared with the reading from an Omega 450 AET thermocouple thermometer at room temperature and at the ice point. At the ice point the dc millivolt amplifier was adjusted to give a 0.00 mV output on the HP 3478A multimeter. Additionally, the thermocouple was dipped in boiling nitrogen at atmospheric pressure as a second check on the accuracy of the reading.

An additional method of determining the temperature was based on the assumption that that the system was in thermal equilibrium and a comparison the vacuum gage readings to tabulated values of temperature from a vapor pressure versus temperature table [Ref. 33: p.367].

Data collection and graphic display of the experiment were controlled by a program in the HP 86B computer. Input devices (voltmeter and multimeter) and output devices (HP "thinkjet" printer, HP 7470A plotter) as well as the HP 9121 disk drive and the HP

82913A monitor were all interfaced to the computer via the HP-IB interface bus. Data and the control program were resident on a hard disk. The program was written in HP basic language. Key features of the program included :

- creating data files
- plotting data
- controlling time intervals between data points
- selecting heating or cooling directions
- conversion of thermocouple voltage to Kelvin temperature scale
- hard copy print out of data

A documented copy of the program is included as Appendix B.

Irradiation of the samples was performed at the Omega West Reactor (OWR) facility at the Los Alamos National Laboratory. OWR is a tank type research reactor moderated and cooled by light water, It has a power level of eight megawatts and can produce a neutron flux of 9×10^{13} neutrons/cm^2. A hydraulically driven transfer system delivers samples in three quarter inch aluminum cans to a position in the reactor core. Position 3-E in the core was used for all of the irradiations. Appendix C contains a list of all test positions in the reactor. Table I describes the flux distribution. Samples were cushioned against mechanical shock by filling the containers with quartz wool. A cadmium shielded container was used to shield the sample from thermal neutrons when studying the effects of fast neutrons. Figure 3 [Ref. 34] describe the characteristics of the flux spectrum of OWR.

C. CONDUCT OF EXPERIMENT

$ErBa_2Cu_3O_7$ samples prepared at NRL were tested for magnetic moment using a 900 series VTS suseptometer at the Naval Research Laboratory before being shipped to Monterey. No data was available at the time this report was being written for the $YBa_2Cu_3O_7$ samples.

After the dimensions of the samples were measured, the superconductivity of each sample was verified by observing the Meissner effect. This quick and qualitative procedure eliminated tedious four terminal method checks on samples which, due to processing or handling methods, did not possess superconducting material. It also confirmed results from four terminal method checks.

The Meissner effect was observed by immersing a sample pellet in liquid nitrogen. leaving the upper half of the pellet exposed to the atmosphere. A small chip of magnet

was then placed over the sample and observed for evidence of levitation. In all of the trials the magnetic chip was approximately 1 mm^3. Particular care was required to ensure that the upper surface of the sample was not wetted by the liquid nitrogen. When the surface was wet, the surface tension of the nitrogen kept the chip from levitating. After the check for the Meissner effect leads were attached to the pellet in the manner described above and a calibration check of the thermocouple was done.

The dewar was prepared by filling it with liquid nitrogen to a depth of 5 cm. The formation of frost on the sample and the leads was considered undesireable. In order to create an inert atmosphere free of water vapor above the liquid nitrogen, a small amount of it was boiled off. This was accomplished by inserting a thick aluminum rod at room tenperature into the liquid nitrogen. A disc with a 0.5 cm vent hole was affixed to the rod to cover the top of the dewar. Sufficient gas was generated to displace the water saturated air and provide the dry inert atmosphere when the warm rod was placed in the liquid nitrogen.

When the control program was started, the resistance versus temperature axes and headings were drawn by the plotter and data collection started. It was imperative to lower the CMS slowly into the dewar in order to minimize the generation of thermal emf in the wires. Careful observation of the HP 3456A digital voltage readout during the lowering process was required to avoid spurious voltage shifts. As soon as the CMS was fully inserted in the dewar, the cork stopper was inserted and the excess nitrogen gas permitted to vent off through the unattached vacuum hose. The stopper was sealed with modeling compound when the sample temperature was approximately 160 K and after the violent boiling terminated. The temperature of the sample was monitored on the HP 3478A. When it appeared that the temperature had stablilized and could go no lower, the dewar was connected to the vacuum system and the pressure inside decreased at a rate of 2.5 mm Hg second to 300 mm Hg. If the initial liquid nitrogen level was low, a considerable amount of time was required to permit the sample to cool to 70 K. The control program was designed to collect a maximum of 200 data points with three seconds between each data point. On some trials data collection would cease after 10 minutes and before the sample had reached 70 K. This situation was averted by manually causing program execution to pause then allowing it to continue on when sample temperature had decreased sufficiently.

Data collection was terminated, the vacuum broken and CMS removed from the dewar upon reaching 70 K. For samples that required immediate subsequent trials, the CMS was placed in physical contact with several lead bricks heated to 330 K.

When sufficient pre-irradiation data was collected on a sample, the leads were removed and excess ECC and thermal compound removed. For shipment to Los Alamos, each sample was individually packaged in shock resistant "bubble wrap" with dessicant in an air tight plastic case.

The first irradiation one pellet of Y-Ba-Cu-O HTS and one pellet of Er-Ba-Cu-O was for 48 minutes in a fast and thermal neutron flux of 1.8×10^{14} neutrons/cm^2. The second irradiation was for like samples but this time for 8 hours corresponding to a total fast and thermal neutron fluence of 5.2×10^{18} neutrons/cm^2. The third irradiation was done on the similiar samples of HTS for seven hours but this shielded by a .16 cm thick cadmium container which permitted only neutrons with energies greater than approximately 0.4 Mev to bombard the sample.

After irradiation, samples were retained at Los Alamos until the activity levels were less than 5 milliroentgens on contact then air shipped to Monterey. The activities of the samples were checked upon arrival at NPS and prior to each trial using an AN PDR-27 radiation detector and stored in a shielded container when not in use. The tests described above were repeated to determine the radiation effects on bulk superconducting transition temperature.

In addition to the tests mentioned thus far, a critical current measurement was attempted on one sample. The procedure for the critical current measurement is essentially the same as the four terminal method except that once the superconducting state is reached, the supply current is increased until a critical current is reached at which time superconductivity is destroyed.

D. COMMENTS ON EXPERIMENTAL PROCEDURE

Preparation of HTS material at the site of the experiment shortly before the resistance and Meissner effect tests are conducted would eliminate many of the possible sources of degradation encountered during shipping. Products of the decompostion in air of HTS have been identified by X-ray powder diffraction as $Ba_2 Cu(OH)_6$. $BaCO_3$. CuO and $Y(OH)_3$. Studies of enhanced degradation in air at 313 K saturated with water vapor have shown that bulk decomposition begins at the surface from which microcrystals of $BaCO_3$ grow. [Ref. 35: p. 403]. The process can be reversed by annealing in flowing oxygen which restores the superconducting phase.

Opinions still differ on the optimum method for conducting the four terminal resistance check. The dc method is suseptible to error mainly because the thermal emf generated at the junction of dissimiliar metals is dc. As long as a well designed cold trap can be provided to minimize thermal gradients at the lead-ECC-sample interface, the dc method will suffice. As an added precaution against thermal emf, the dc supply current should be reversed and the average of the two voltage measurements taken to eliminate the thermal emf effects. If the sample's room temperature voltage drop is extremely small due to sample size or lead contact configuration, consideration should be given to using the ac four terminal test. Use of an ac current source with a lock in amplifier avoids the dc thermal emf but is suseptible to errors due to stray inductance and capacitance in the system.

The design of the cryogenic system fulfills the low temperature and inert atmosphere requirements for this type of work. Greater flexibility and automation of the experiment could be realized if a heating element was added to the CMS. This would permit control of the heating or cooling rates. The method of attaching leads with ECC was often tedious but superior to the indium soldering method reported by Sweigard [Ref. 36] in that lead contact was assured trial after trial. The geometry of the HTS samples precluded accurate determination of the length and area of the conductor required for the actual calculation of the resistivity. Therefore, data was recorded as the voltage drop across an arbitrary path of current on the sample. Once the expertise is developed to process the samples into bars of other regular shapes by machining, the conversion of voltage to resistivity can be accomplished easily by computer calculation.

A further improvement to the computer program would be to make it more "user friendly". In its current configuration selection of options such as data collection time intervals, thermocouple conversion equations and direction of temperature change must be made by manual revision of the program.

It is believed that a consistant error in measurement of the sample existed. The thermocouple consistently measured the temperature of boiling nitrogen at atmospheric pressure at 82 K vice the accepted value of 77 K. Likewise, at a pressure of 300 mm Hg, corresponding to a temperature of 70 K, the thermocouple meter read 75 K. These low temperatures were at the limits of the thermocouple's range of accuracy.

Several factors were considered in determining the energy and fluence ofthe neutron irradiation. Since one of the goals of the experiment was to understand behavior of HTS subjected to nuclear weapons, energies and fluences of neutrons on the order of those

from fission were selected for study. Figure 4 [Ref. 26: p. 363] illustrates the neutron energy spectrum resulting from a fission weapon. Figure 5 [Ref. 27: p. 365] shows the fluence levels resulting from fission weapons. Since the yields of many nuclear weapons are in the megaton range, the fluence indicated on the graph must be multiplied by a factor of three to correspond to the long exposure in this experiment. It is also of interest to note that, for fusion reactors, a lifetime of exposure to fast neutrons of approximately 5 x 10^{18} neutrons/cm^2 is a typical design criteria. [Ref. 37]. In lieu of an actual nuclear weapon test, the requisite neutron flux was provided by the Omega West Reactor. Appendix II contains fluence data for different positions in the reactor. The effects of 14.1 Mev neutrons, characteristic of thermonuclear reactions, were not studied because no source was readily available at the time of the experiment.

Maisch et al. [Ref. 28] studied the effects of 63 Mev protons on $YBa_2Cu_3O_7$ at fluence levels of 10^{14} protons/cm^2. They discovered an increase in sample resistance with decreasing temperatures and a loss of superconductivity.Figure 6 shows their results for various proton fluxes. They attributed these effects to oxygen disorder. X-ray diffraction of irradiated samples indicated that no phase change occurred, i.e. the sample did not transition from octahedral to tetragonal structure.

Atobe et al. studied the effects of neutrons on $YBa_2Cu_3O_7$ at 20 K but found that while there was a shift in T_c to a lower temperature after being exposed to a fluence of 10^{14} fast neutrons/cm^2 superconductivity was still achieved. They also observed drastic increases in resistivity. They suggested that the changes in resistivity were due to the formation and breakdown of local paths rather than arising out of bulk structure [Ref. 38].

Sweigard [Ref. 36] conducted electron irradiations on Yttrium and Gadolinium based HTS and found almost imperceptible shifts to lower transition temperatures.

IV. EXPERIMENTAL RESULTS

A. EXPECTATIONS

Based on the knowledge that the HTS mechanism relies on a highly ordered structure and stoichiometrically precise composition, it was expected that the HTS would experience a shift to lower transition temperatures as a result of exposure to neutron irradiation. The predicted mechanism for this damage was that incident neutrons would disrupt the ordered structure by causing classic damage such as Frenkel defects and thermal spikes. The decrease in the transition temperatures was expected to become more pronounced with increasing neutron fluence and energy. Some shift in the transition temperature was expected. It was believed that by the time the activities of the samples reached safe working levels, a significant amount of the damage would be repaired through the annealing process.Further, despite the presence of some damaged material, it was expected that there would be a perceptible Meissner effect. Earlier reports had speculated on the possibility of minute superconducting chains of HTS material existing throughout the bulk material. Given the typical current density parameter of HTS (10^6 A cm^2) , it might be possible for HTS to carry sizable currents despite being subjected to high fluences and incurring great damage.

B. OBSERVATION AND RESULTS

Tables 2 and 3 summarize the results of the experiment. Samples 1 and 2 were tested for the Meissner effect prior to irradiation but found incapable of levitating the smallest chip of magnet. No further tests were made but they were used to perfect lead wire attachment techniques.

Sample 3 displayed the Meissner effect and a classic transition [Fig. 7]. In an attempt to investigate the critical current, the supply current was gradually increased up to a maximum of 100 mA once the sample had reached the superconducting state. The standard procedures were followed for removing leads prior to packing for shipment to Los Alamos. Unfortunately, while removing the sample from the grease bed, the sample split in half leaving two disks approximately half the thickness of the original disk. In light of the grossly modified geometry and the possibility for further damage during the experiment, the sample was not investigated any further.

Samples 4 and 5 also displayed typical HTS behavior prior to irradiation. Both exhibited strong Meissner effects and had T_c of 88 K and 90 K respectively. Figures 8 and 9 illustrate their response to decreasing temperature.

Despite being exposed to a fluence one order of magnitude less than the other trials, samples 4 and 5 were found to be reduced from pellets to powder upon removal from the reactor. The samples were retained at Los Alamos and no further tests conducted.

Useable pre-irradiation data were obtained for samples 6 and 7. The Meissner effect was clearly evident, levitation was strong and unmistakable. T_c was found to be sharp and complete at 87 K and 76 K respectively. In short, they displayed classic behavior for a well formed HTS. Figures 10 and 11 illustrate the relationship between voltage drop and temperature. After exposure to a fast and thermal neutron fluence of 10^{18} neutrons / cm^2 with an annealing time of 30 days, no Meissner effect was observed in either sample. Both samples required considerably less current to achieve a voltage drop equal to pre-irradiation values. Significantly, the magnitude of the voltage drop continued to increase with decreasing temperature [Fig. 12]. For sample 6, a small broad transition was observed at 81 K but the superconducting state could not be achieved. The behavior of sample 7 was quite similiar with the exception that it did not exhibit any transition whatsoever. Figure 13 illustrates the response to decreasing temperature. Figure 14 shows the response after an annealing time of 60 days at room temperature.

Samples 8 and 9 were both produced at NRL. They displayed a distinct Meissner effect prior to irradiation. Both samples exhibited sharp transitions to the superconducting state at 88 K and 83 K respectively [Figs. 15 and 16]. The anomalous knee present in the approach to superconductivity occurred during a momentary loss of vacuum caused by the vacuum hose slipping off the tee connection. Once the tube was reattached, the equilibrium superconducting state was attained. The samples were placed in 0.16 cm thick cadmium container and irradiated in core position 3-E for seven hours. This resulted in a total fast neutron fluence of 2.2 x 10^{18} neutrons/ cm^2 . Placing the samples in a cadmium container subjected them to a significant gamma heating in excess of 5 W/g [App. C]. Since the mass of the samples was approximately 32 g , the temperature was likely very high. Post-irradiation inspection revealed several hairline cracks in both samples. Immediately evident was a rusty orange discoloration of the yttrium sample. After irradiation neither sample exhibited the Meissner effect despite repeated trials with a minute chip of magnet. As a check, the same magnetic chip was levitated by an unirradiated sample of Er-Ba-Cu-O. The texture of sample 8 was very crumbly.

As in other irradiated samples, a much smaller current produced greater voltage drop. Less than 1 mA was required to obtain a voltage drop of 50 mV. Examination of Figure 17 reveals that the sample did not reach the superconducting state. In contrast to samples 6 and 7, the voltage decreased with decreasing temperature. Full examination of this trend was precluded by the inability to attain temperatures lower than 70 K. Also significant is the absence of spurious voltages in the initial cooling phase. Severe cracking of sample 3 was observed upon removal from the dewar. The severity of the damage can be noted in Figure 3. The excess thermoconductive grease and dark orange discoloration were scraped from the yttrium sample before the leads were attached in the standard manner. No spurious voltages in the voltage vs. temperature trace were observed. Figure 18 demonstrates that the resistivity of the sample increased linearly with decreasing temperature. The severe cracking observed in sample 8 did not occur in sample 9. It remained intact after the resistivity measurement.

V. CONCLUSIONS AND RECOMMENDATIONS

A. EXPERIMENTAL CONCLUSIONS

As the result of this experiment, the following conclusions can be drawn:

- The superconducting properties of Y-Ba-Cu-O and Er-Ba-Cu-O HTS are destroyed by neutron irradiation on the order of 10^{18} neutrons/cm^2. In fact, in terms of resistivity, post-irradiation behavior resembles that of metals. Sample resistivity increased as temperatures were lowered to the liquid nitrogen regime and superconductivity was not attained. The postulated reason for this behavior is that the highly ordered Cu-O chains in the orthorhombic lattice were disrupted by neutron displacement damage and subsequent lattice distortion. Atomic displacements may have interfered with any conduction mechanism relying on electron-phonon interactions. Similiar results were obtained by Maisch et al. and Atobe et al..

- The performance of high temperature superconductors is strongly reliant on precise stoichiometry. The fact that samples 1 and 2 received the same processing as other samples which were superconducting indicates that perhaps the incorrect amounts of constituent powders were weighed out during preparation.

- The samples tested showed no evidence of low temperature annealing after irradiation. Despite a period of over two months, during which defects could have annealed, no such process was observed to occur. In light of the serious defects observed in the samples, radiation damage was regarded as severe in this experiment.

- Failure of the HTS sample involved in the critical current measurement was due to thermal stress. Despite the fact that failure was after a critical current measurement, catastrophic failure due to exceeding the critical current can be ruled out. The large size of the sample and the small current make it unlikely that the typical value of 10^6 A / cm^2 could be exceeded.The samples used were not dense (typically on the order of 80 % of the theoretical value of 6.38 g / cm^3 for yttrium HTS) and brittle. The thermal stress of rapid cooling likely was the cause of the cracking. This is consistent with the knowledge that ceramics are sensitive to thermal shock.[Ref. 25: p. 214]

- The reduction of samples 4 and 5 to powder was most likely due to thermal stress. The samples could have been in a position in the core which was subject to a high level of gamma heating.

- The absence of spurious voltages during the initial cooling phase in samples 8 and 9 was due to the reduction of thermal emf. Taping the copper wires to the side of the sample holder had the effect of making the CMS into a more efficient cold trap.

- The severe cracking in sample 8 was due to thermal stress. Hairline cracks initially caused by gamma heating and possible lattice dimension changes increased greatly in size and number after the post-irradiation resistivity measurement. The decrease in resistivity with decreasing temperature should be considered invalid due to considerable mechanical damage to the sample.

- The discoloration of sample 9 was was a manifestation dislocation damage. This same effect has been observed in other ceramic materials. Dienes [Ref. 39: p. 80] attributes this to a change in the density of color centers.

B. RECOMMENDATIONS

The conduct and evaluation of this experiment over several months generated suggestions for improvements in methods and equipment as well as new areas for investigation.

- The experiment clearly established that Y-Ba-Cu-O and Er-Ba-Cu-O HTS suffer significant and irreversible loss of superconductivity in the absence of post irradiation high temperature / oxygen atmosphere annealing. Future work should be aimed at establishing the threshold levels of irradiation required to cause loss of superconductivity in HTS in the liquid nitrogen temperature regime.
- The role of lattice distortion (due to exposure to fast particle fluxes) and its effect on Cu-O ordering should be investigated.
- Development of HTS should take into account the suseptibility to radiation damage. Given different materials with approximately equal transition temperatures and critical fields and currents, the one selected for use should be the one with the lowest total cross section for interaction with incident radiation.
- The ac four terminal method for determing resistivity should be adopted as standard practice. Use of a low frequency ac signal with a lock-in amplifier should eliminate thermal emf transients during the rapid initial cooling phase of the measurement. In lieu of this technique, taping leads to the sample holder will significantly reduce the unwanted thermal emf.
- Determination of bulk superconductivity by observing levitation of a magnet is qualitative in nature. Use of a susceptometer before and after irradiation would provide a better measure of bulk superconductivity.
- Better temperature control of the CMS and the sample could be achieved by adding a strip heater to the CMS and integrating it into the computer control system.
- Use of a different type of thermocouple with a wider temperature range of operation may help to avoid the consistent error experienced at the low end of the temperature measurement.
- Although the ECC method of attaching terminal leads was satisfactory, it is a tedious method. The emerging standard method of attachment is ultrasonic soldering of indium. The ultrasonic method of soldering leads should be used.
- Proficiency in producing HTS locally should be developed as should the ability to machine the material into shapes with enough symmetry to permit the calculation of the resistivity.

APPENDIX A. FIGURES

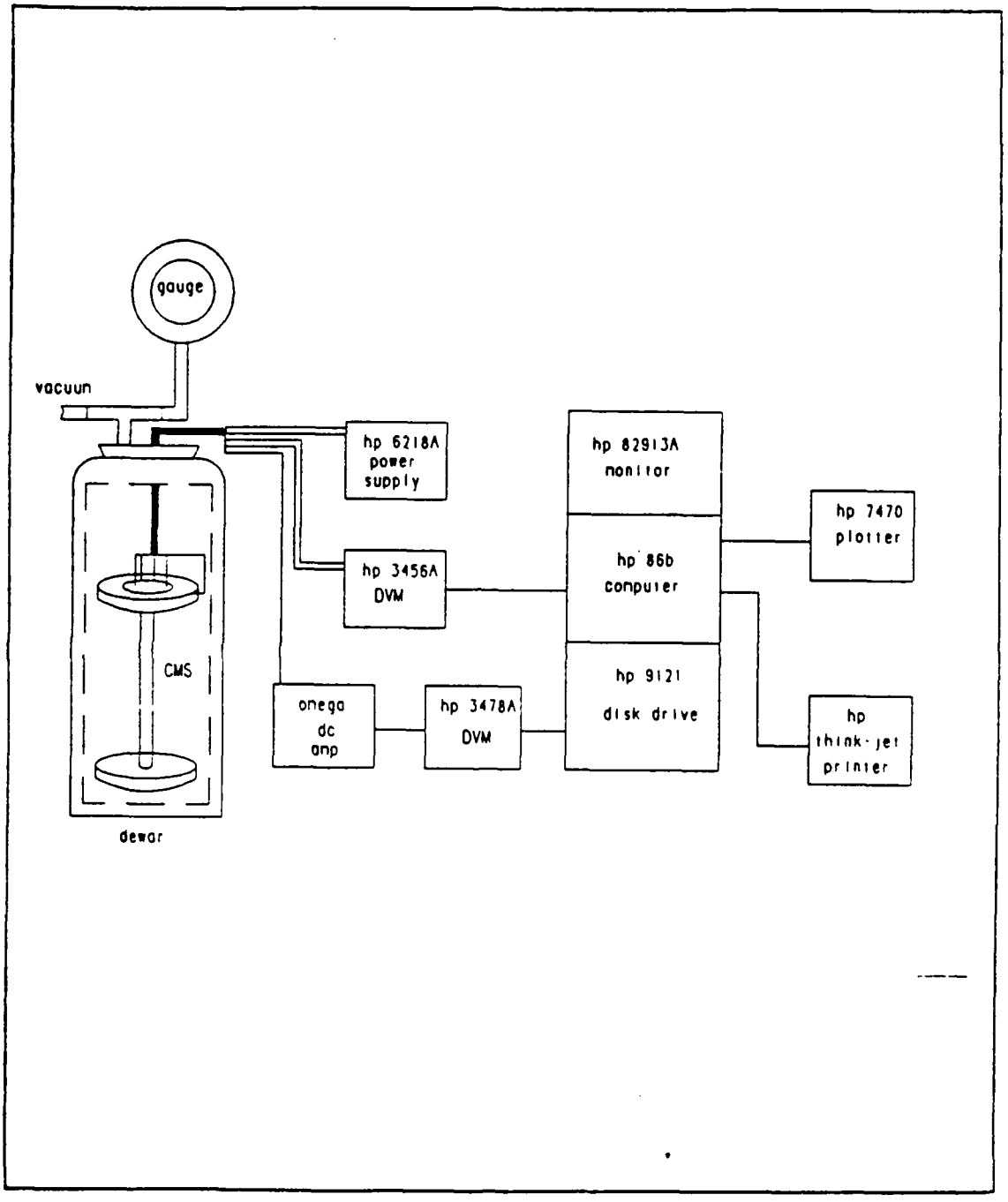

Figure 1. Block Diagram of Resistivity Measurement System

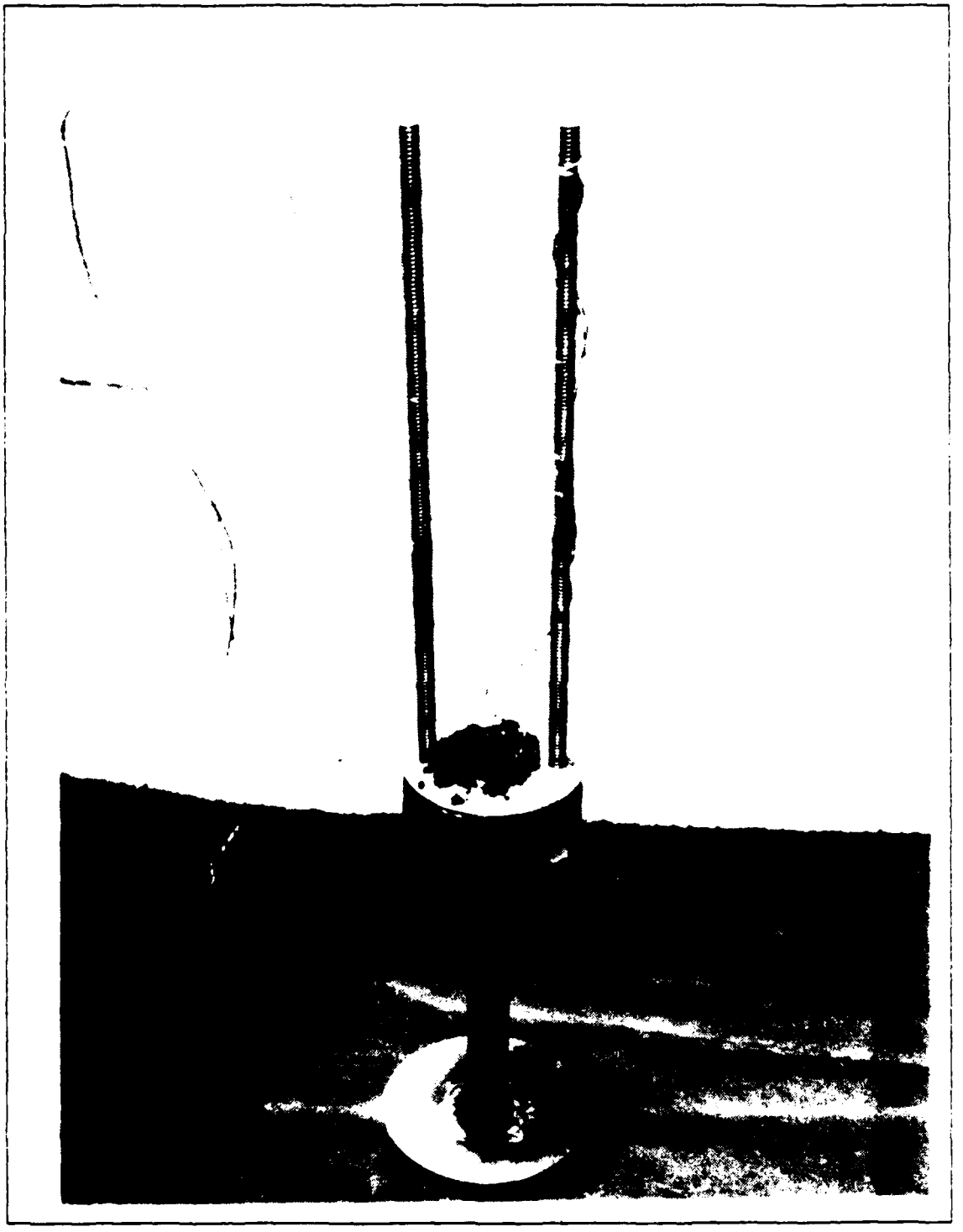

Figure 2. Cryogenic Mounting Stand (CMS)

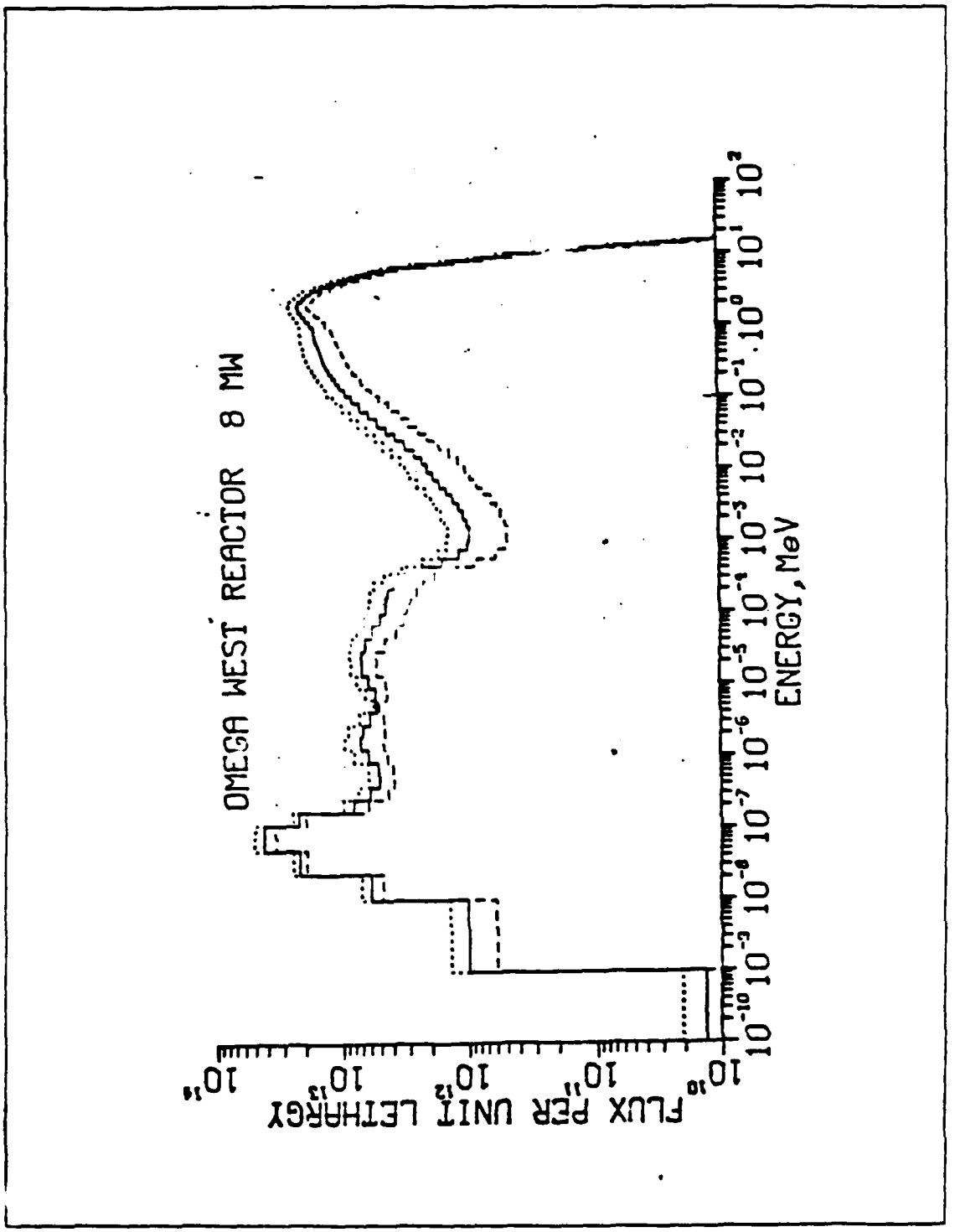

Figure 3. Flux Spectrum of the Omega West Reactor: (Ref. 34)

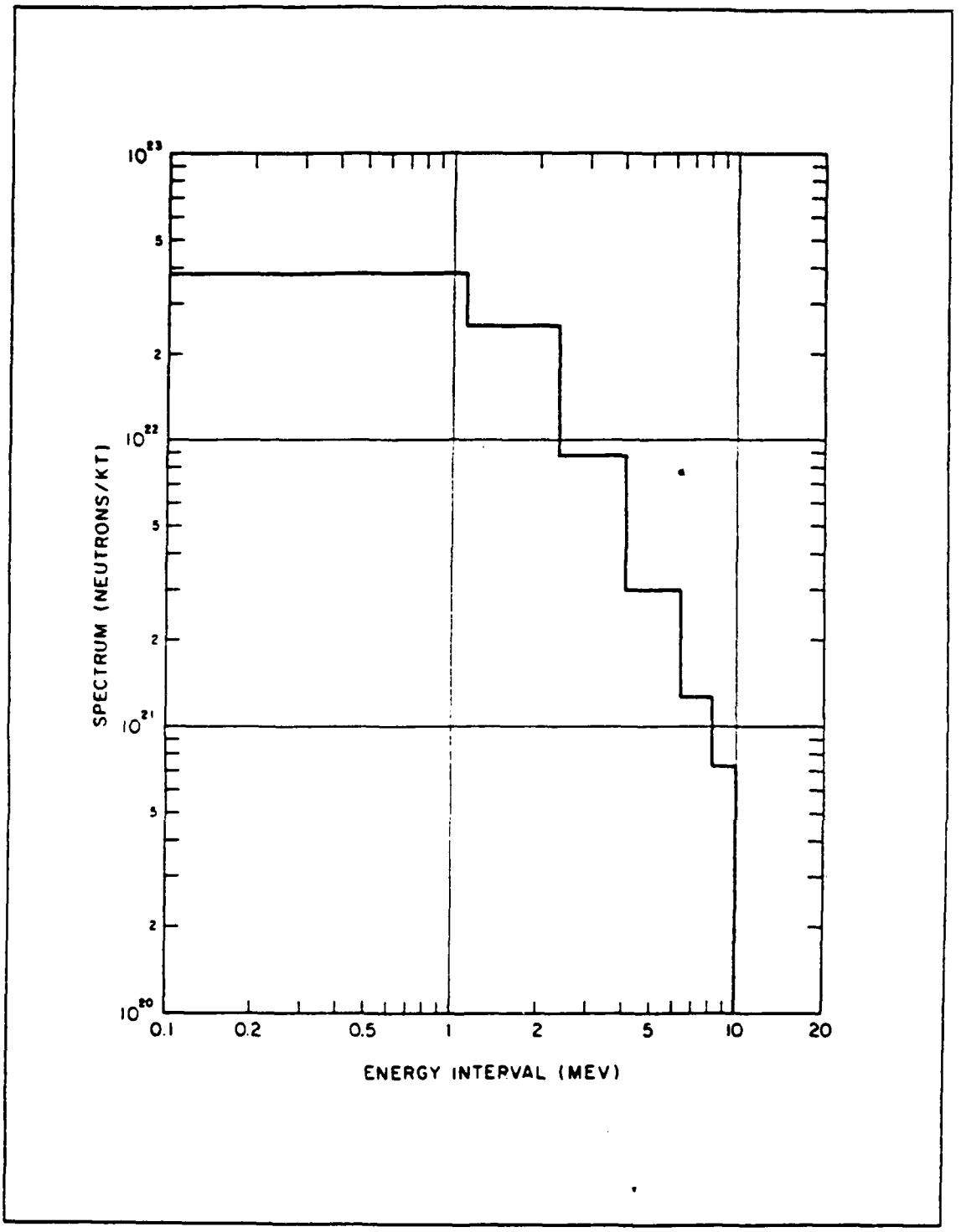

Figure 4. Fission Weapon Neutron Energy Spectrum: (Ref. 26)

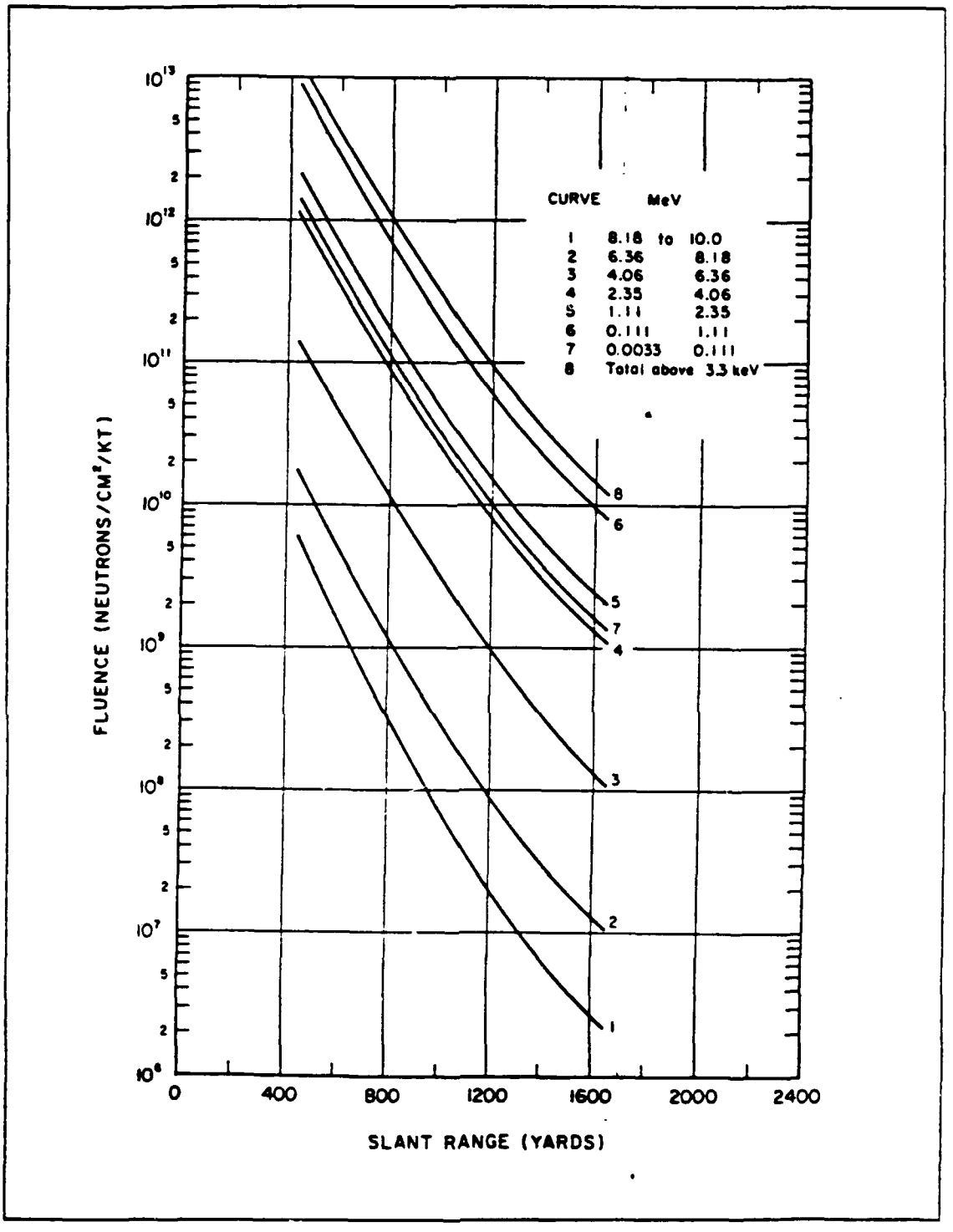

Figure 5. Fission Weapon Neutron Fluence Levels: (Ref. 26)

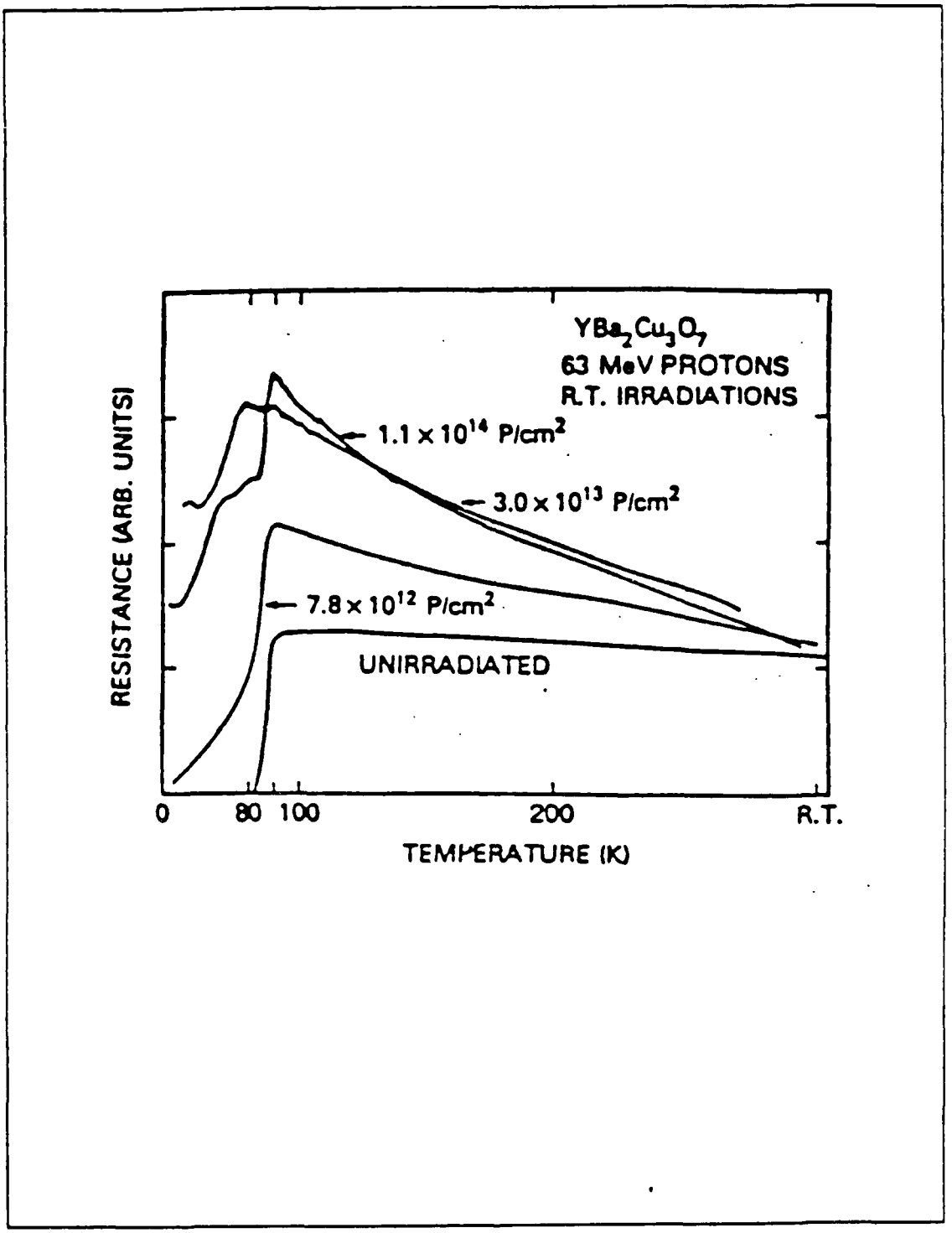

Figure 6. Resistivity of Electron and Proton Irradiated HTS: (Ref. 28)

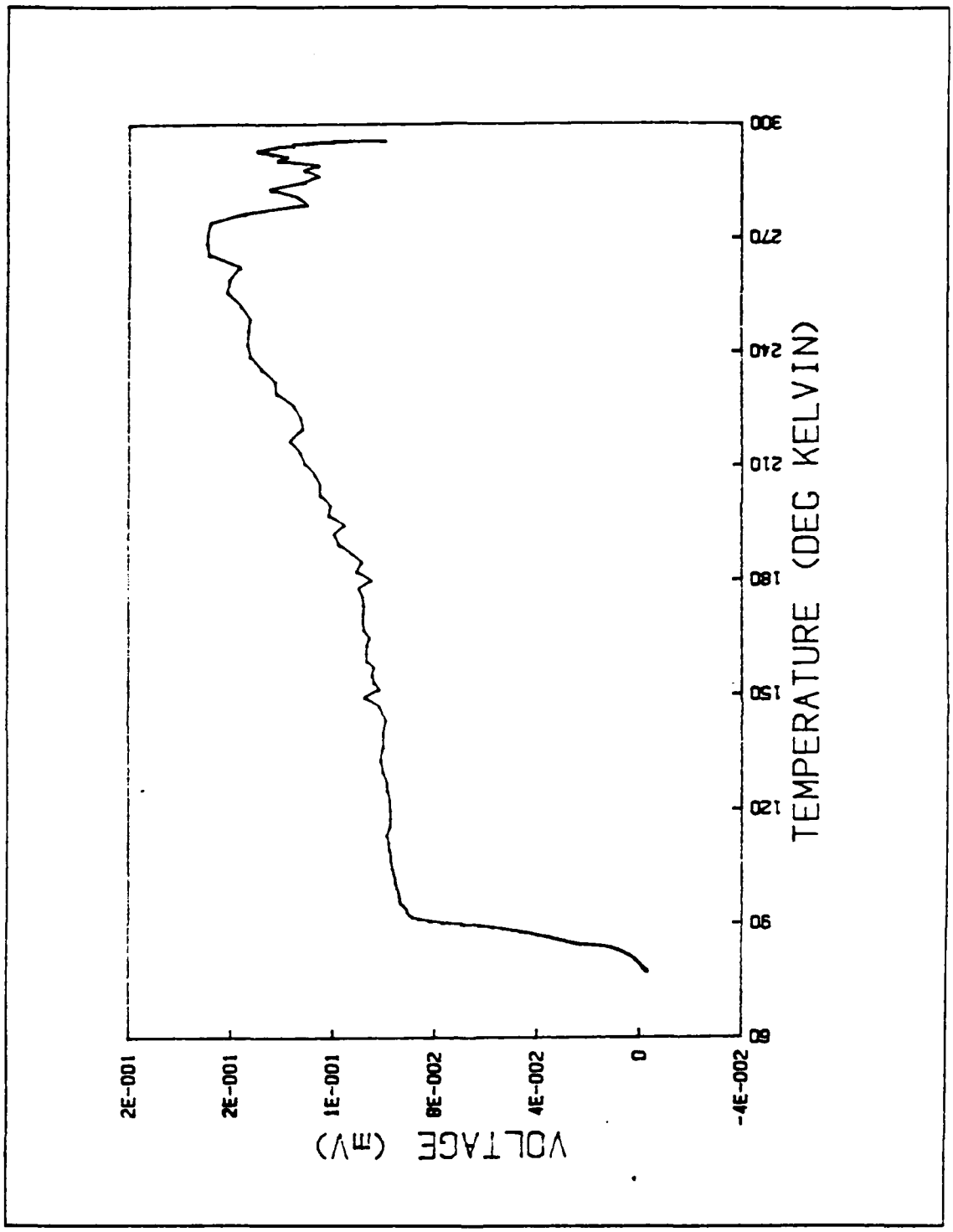

Figure 7. Sample 3 Voltage vs Temperature Curve (Pre-irradiation)

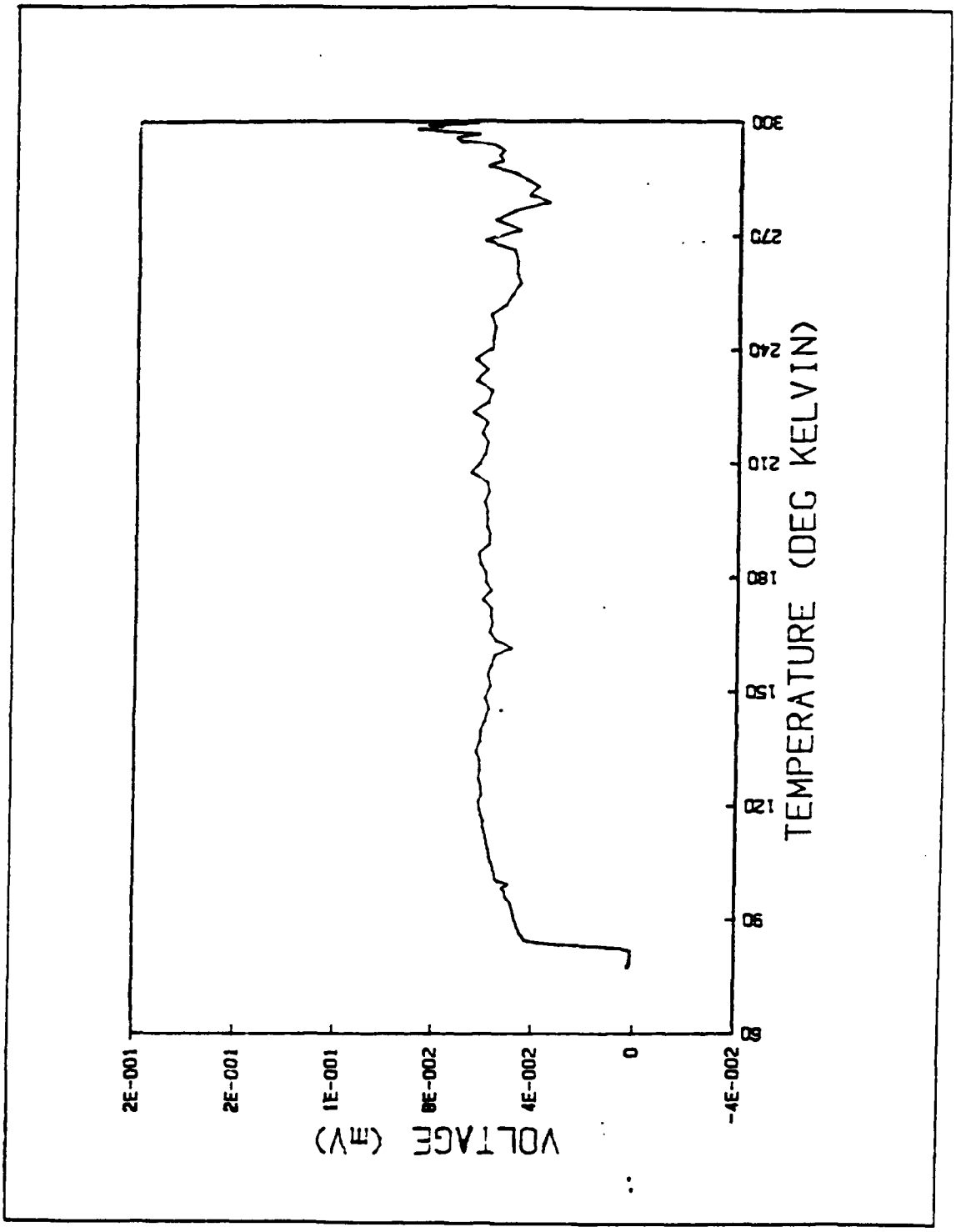

Figure 8. Sample 4 Voltage vs Temperature Curve (Pre-irradiation)

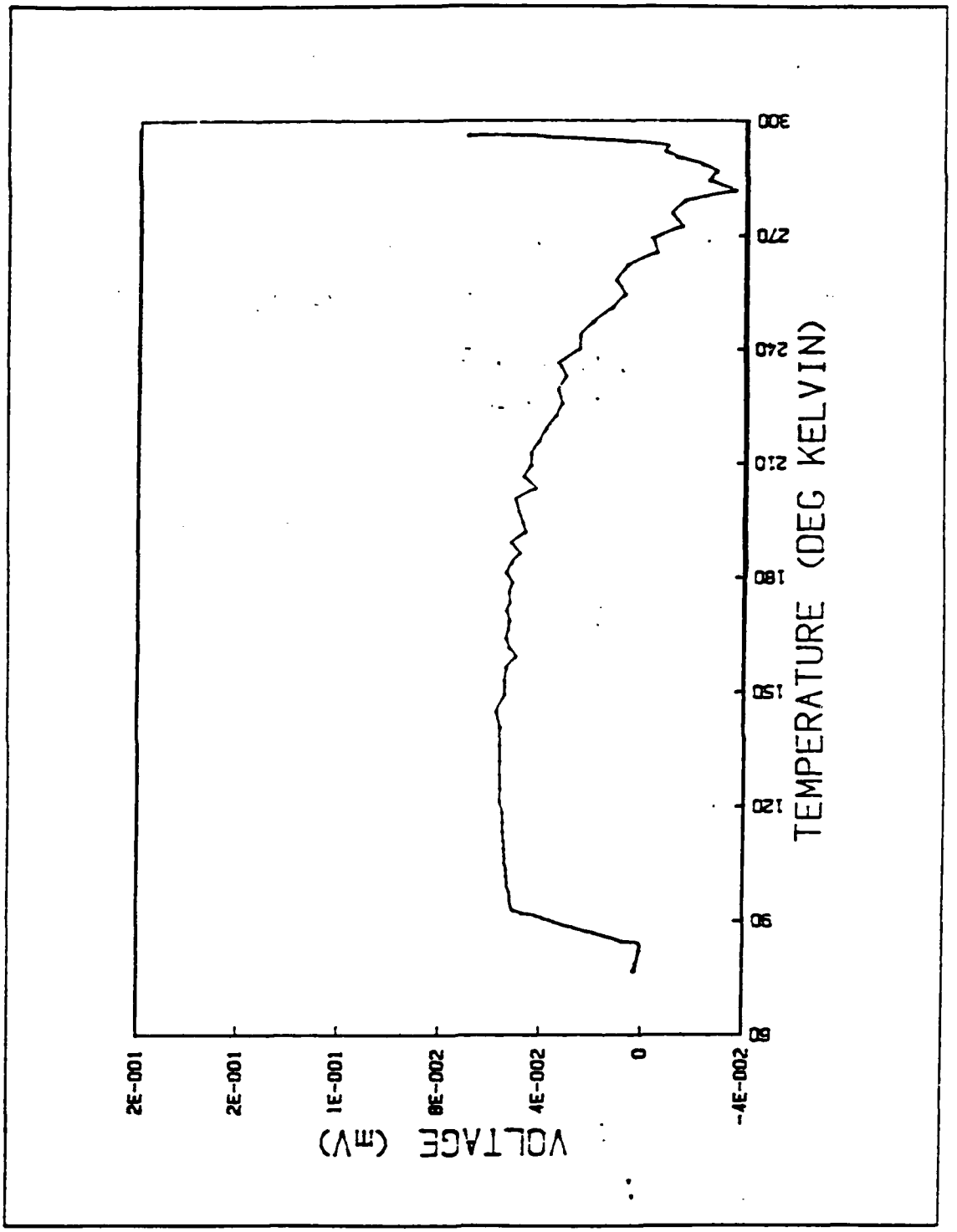

Figure 9. Sample 5 Voltage vs Temperature Curve (Pre-irradiation)

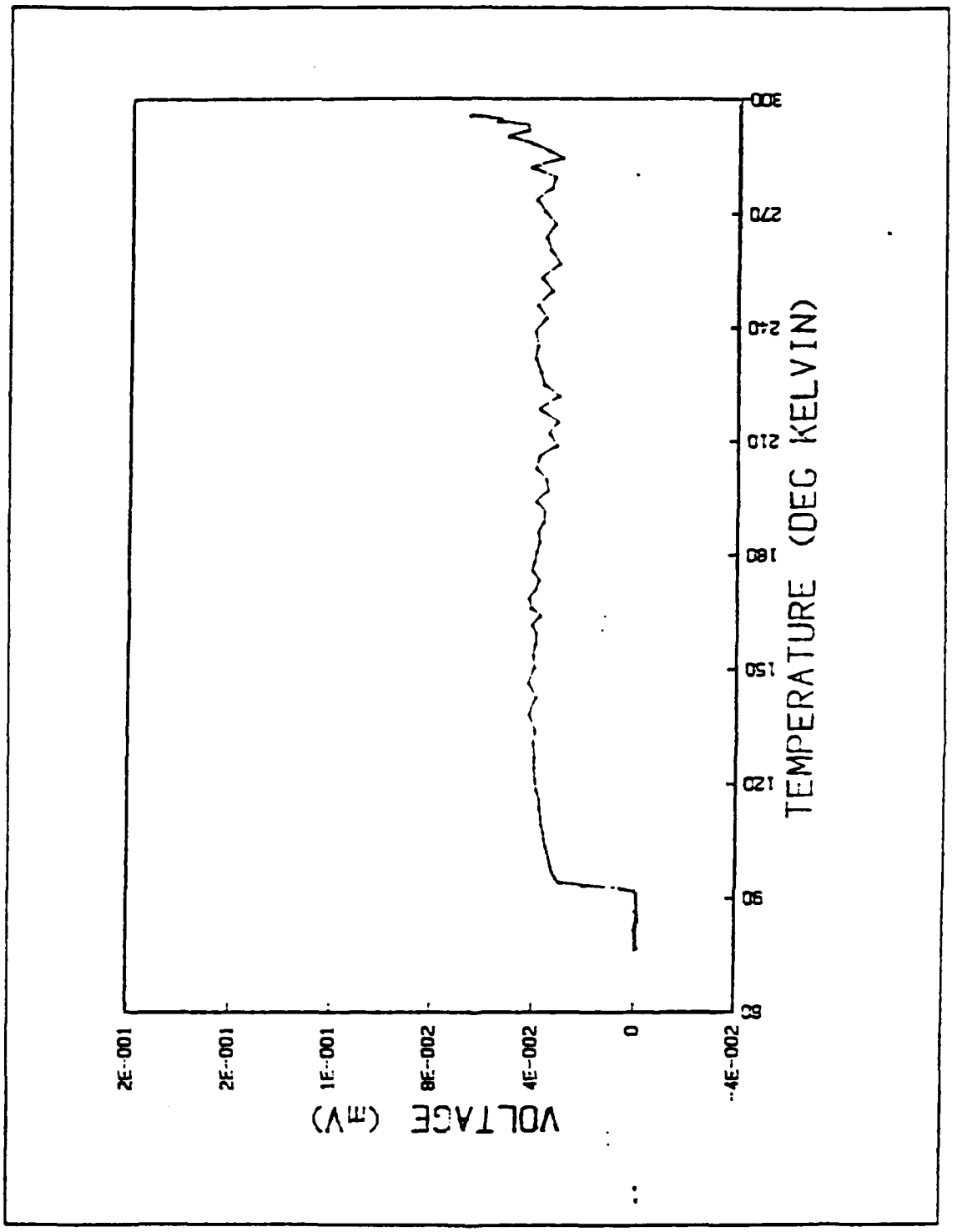

Figure 10. Sample 6 Voltage vs Temperature Curve (Pre-irradiation)

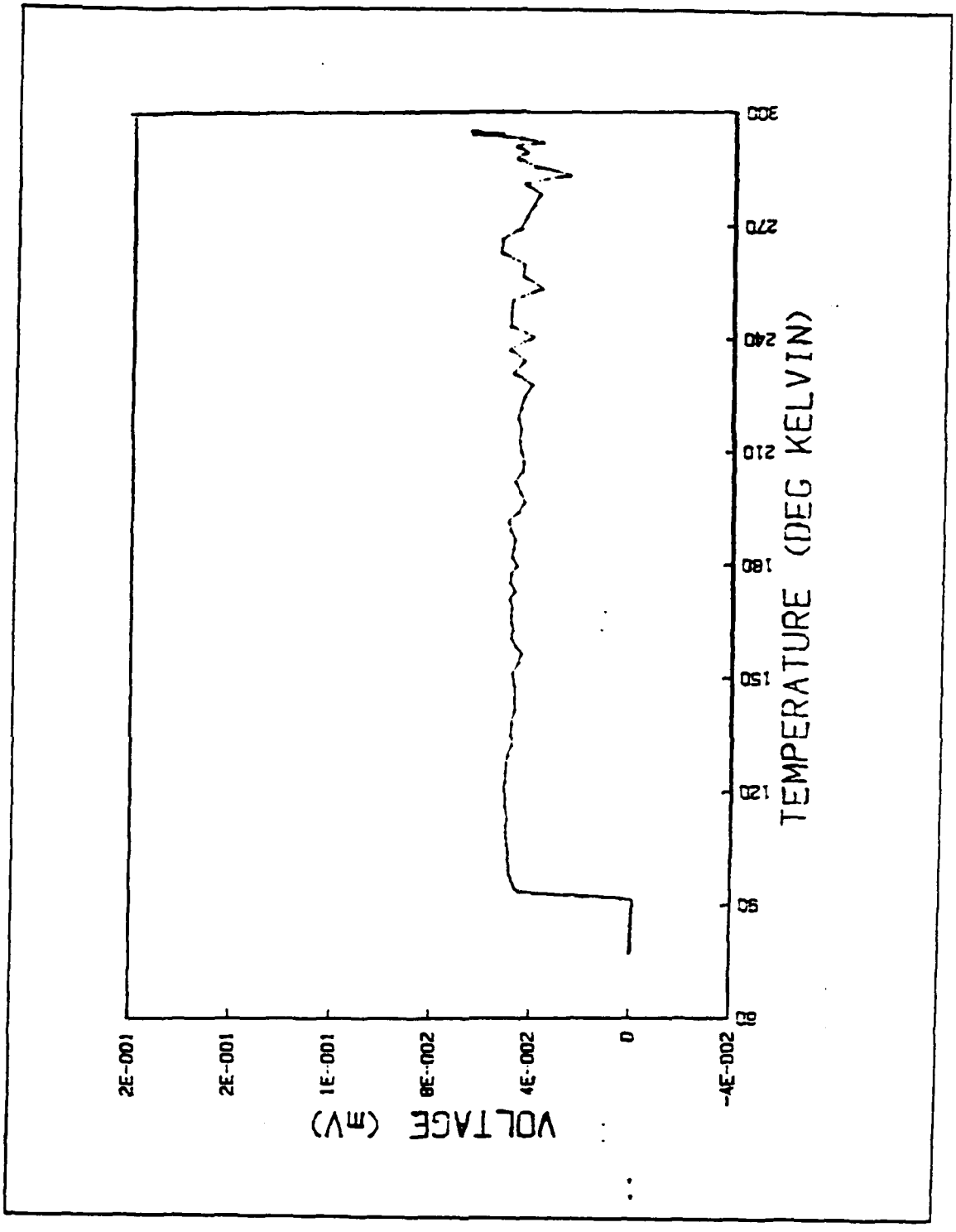

Figure 11. Sample 7 Voltage vs Temperature Curve (Pre-irradiation)

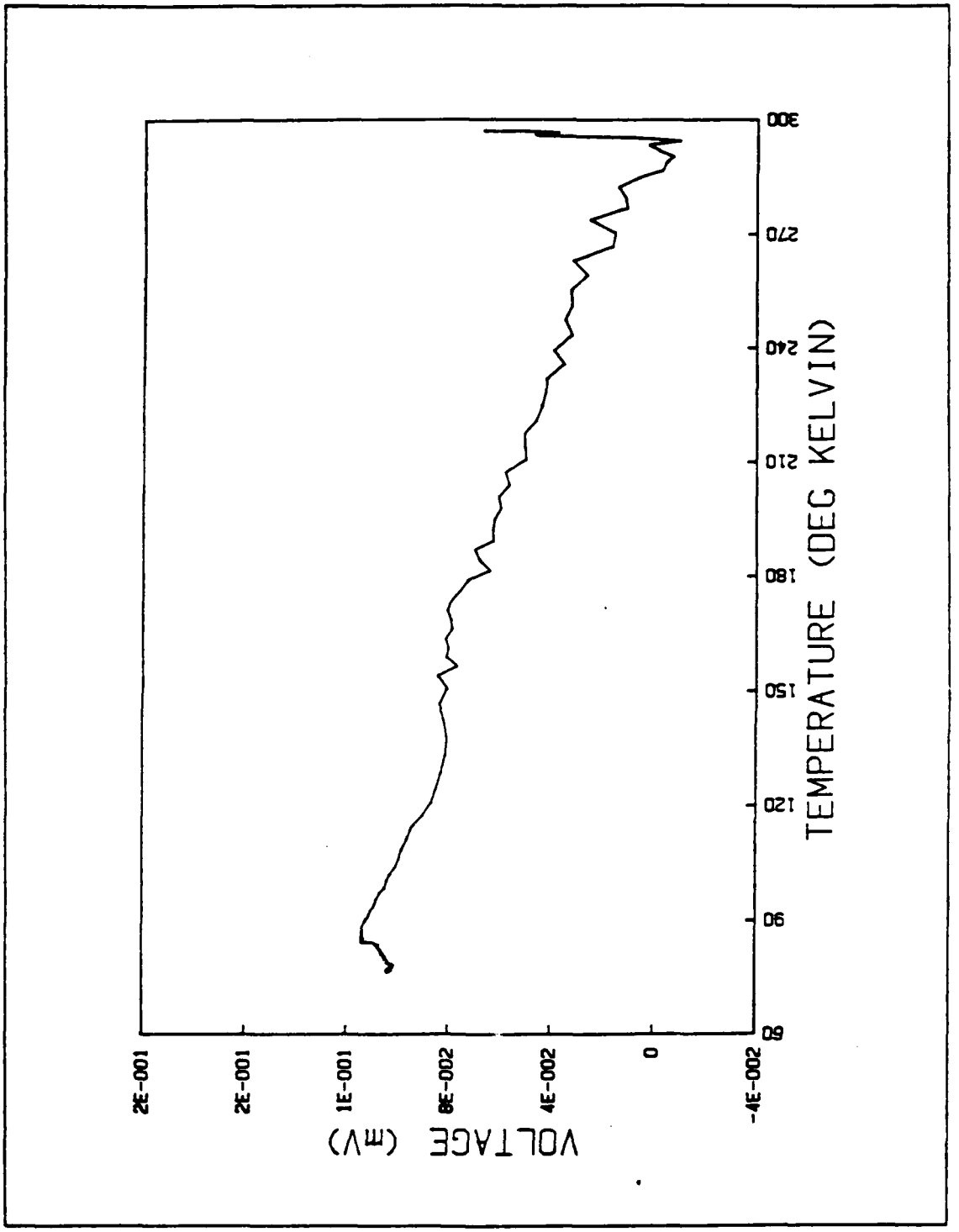

Figure 12. Sample 6 Voltage vs Temperature Curve (Post-irradiation)

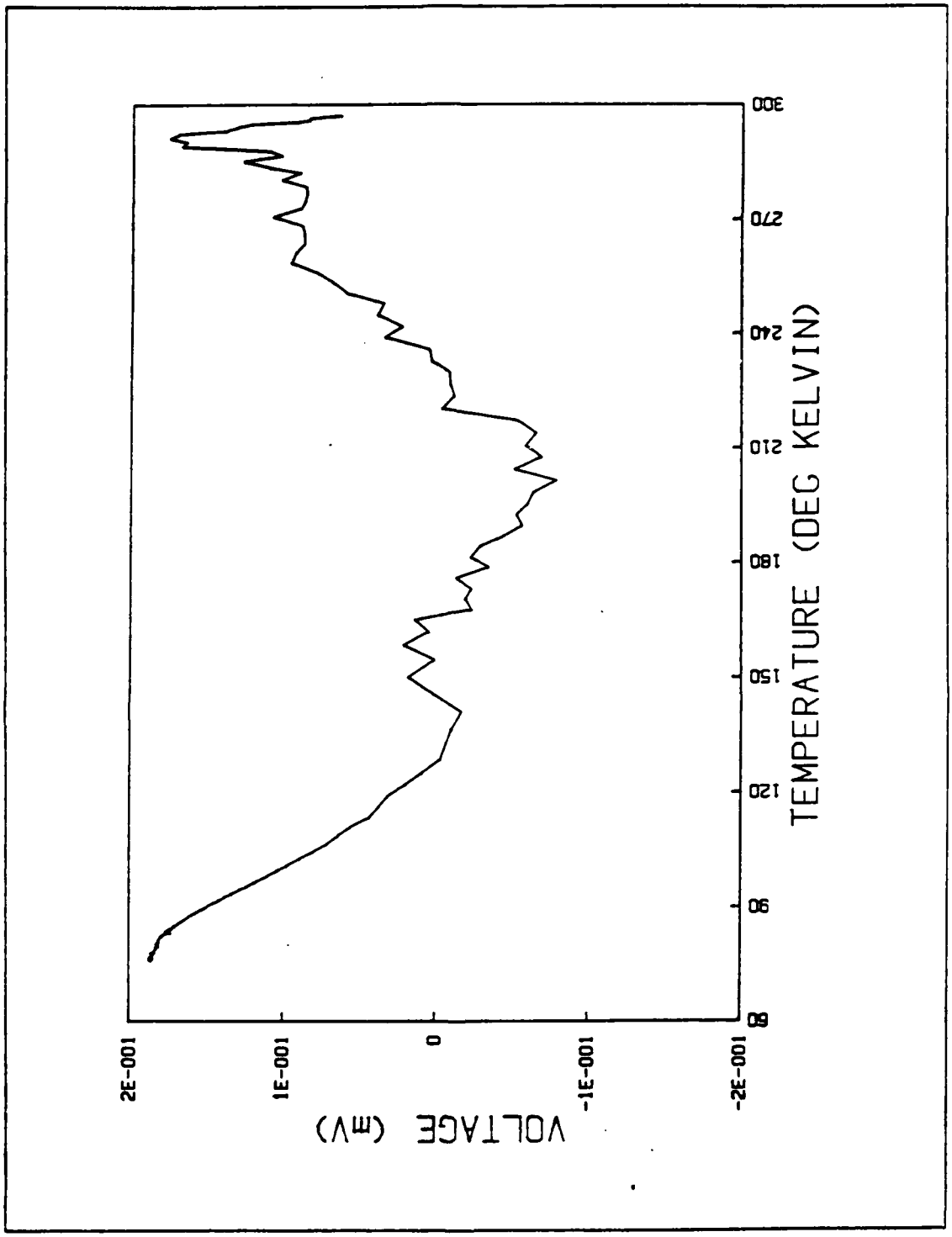

Figure 13. Sample 7 Voltage vs Temperature Curve (Post-irradiation- 30 days)

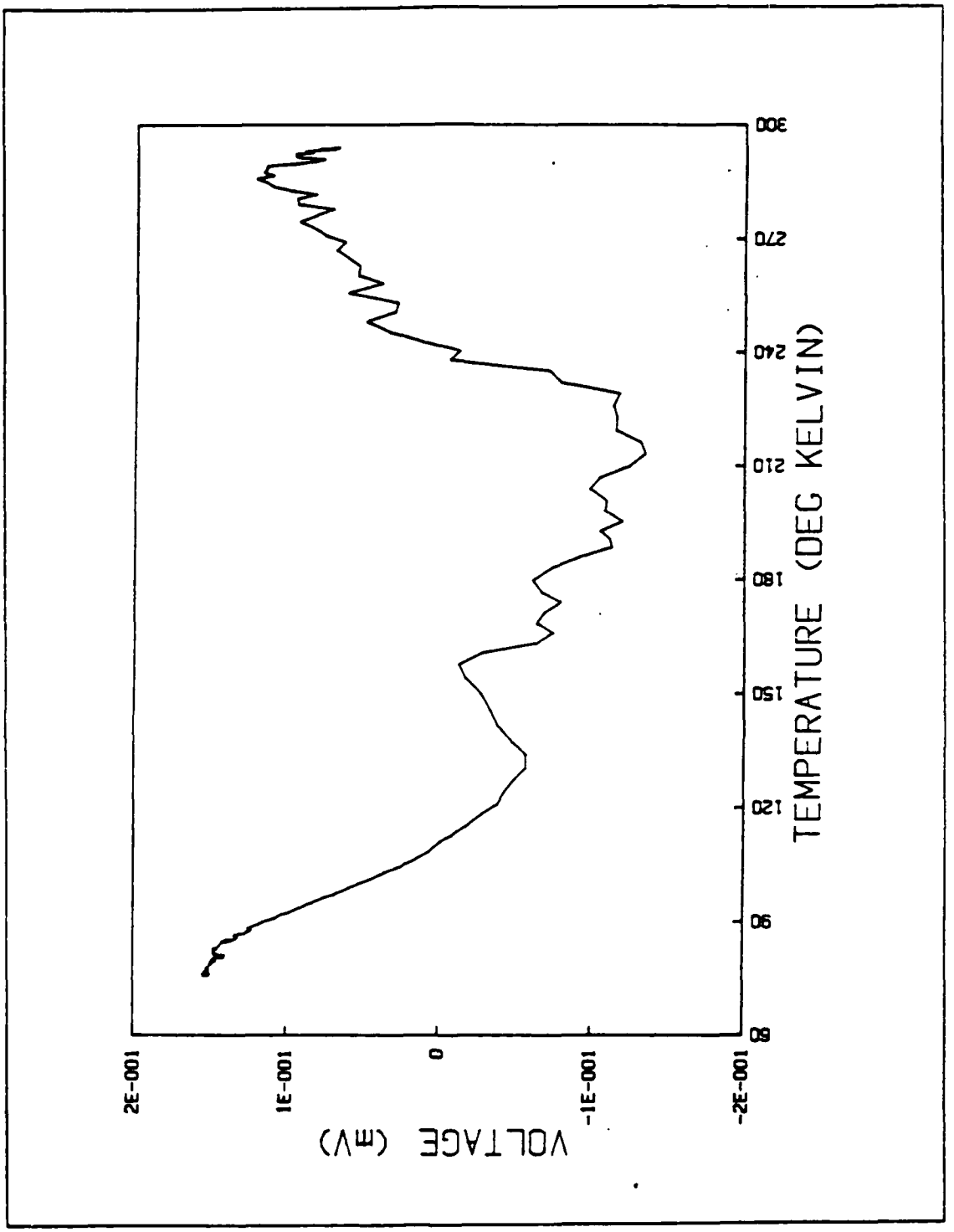

Figure 14. Sample 7 Voltage vs Temperature Curve (Post-irradiation- 60 days)

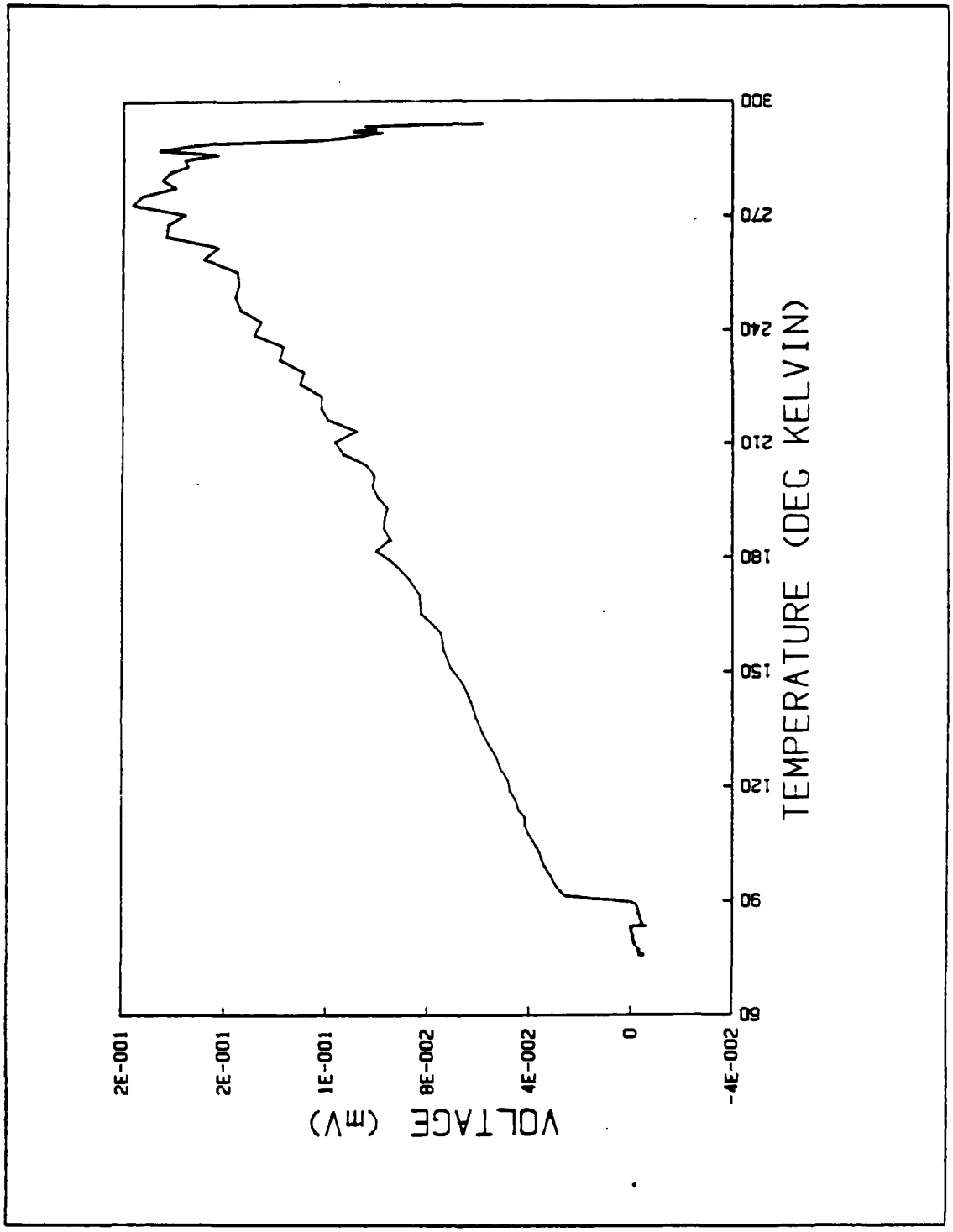

Figure 15. Sample 8 Voltage vs Temperature Curve (Pre-irradiation)

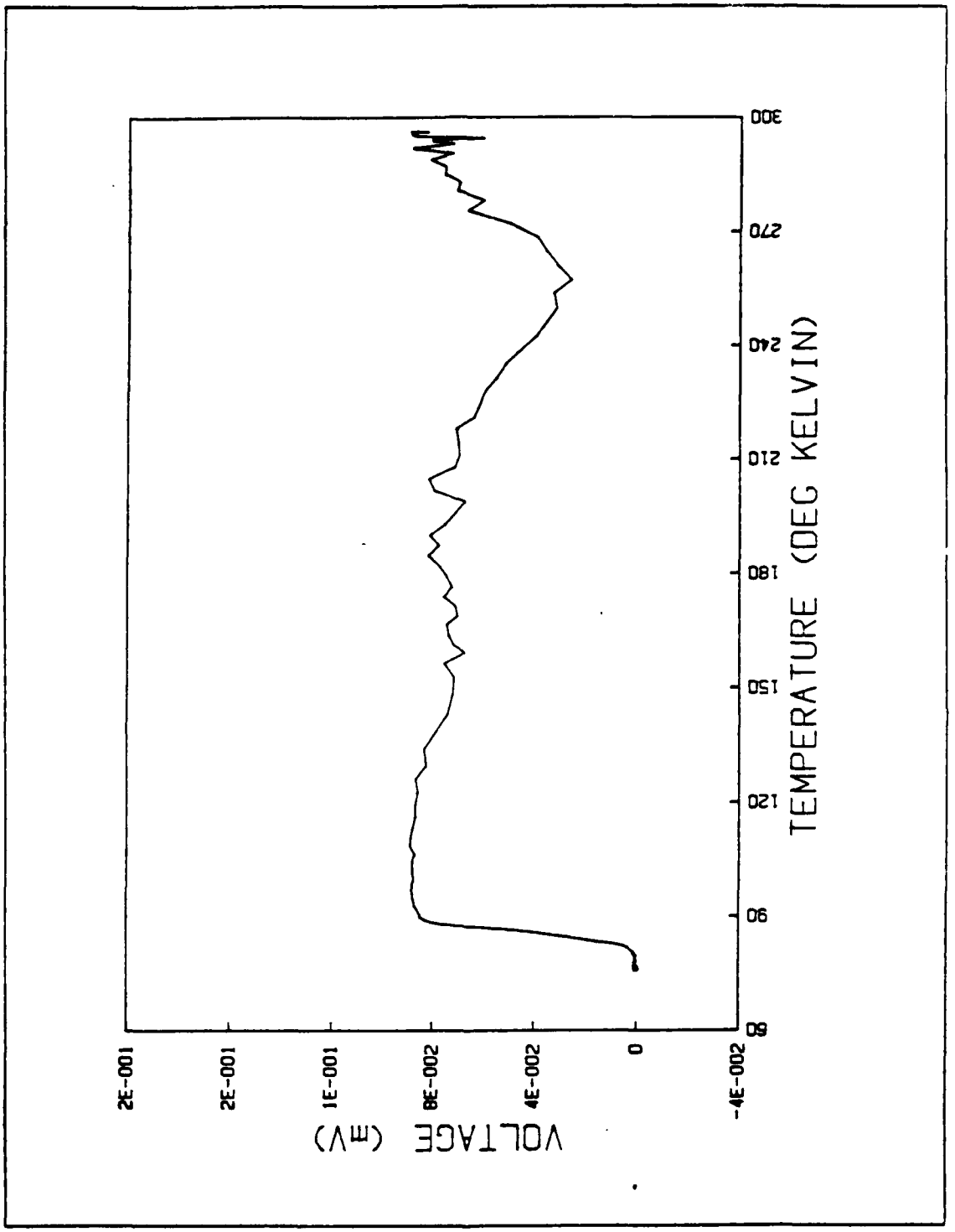

Figure 16. Sample 9 Voltage vs Temperature Curve (Pre-irradiation)

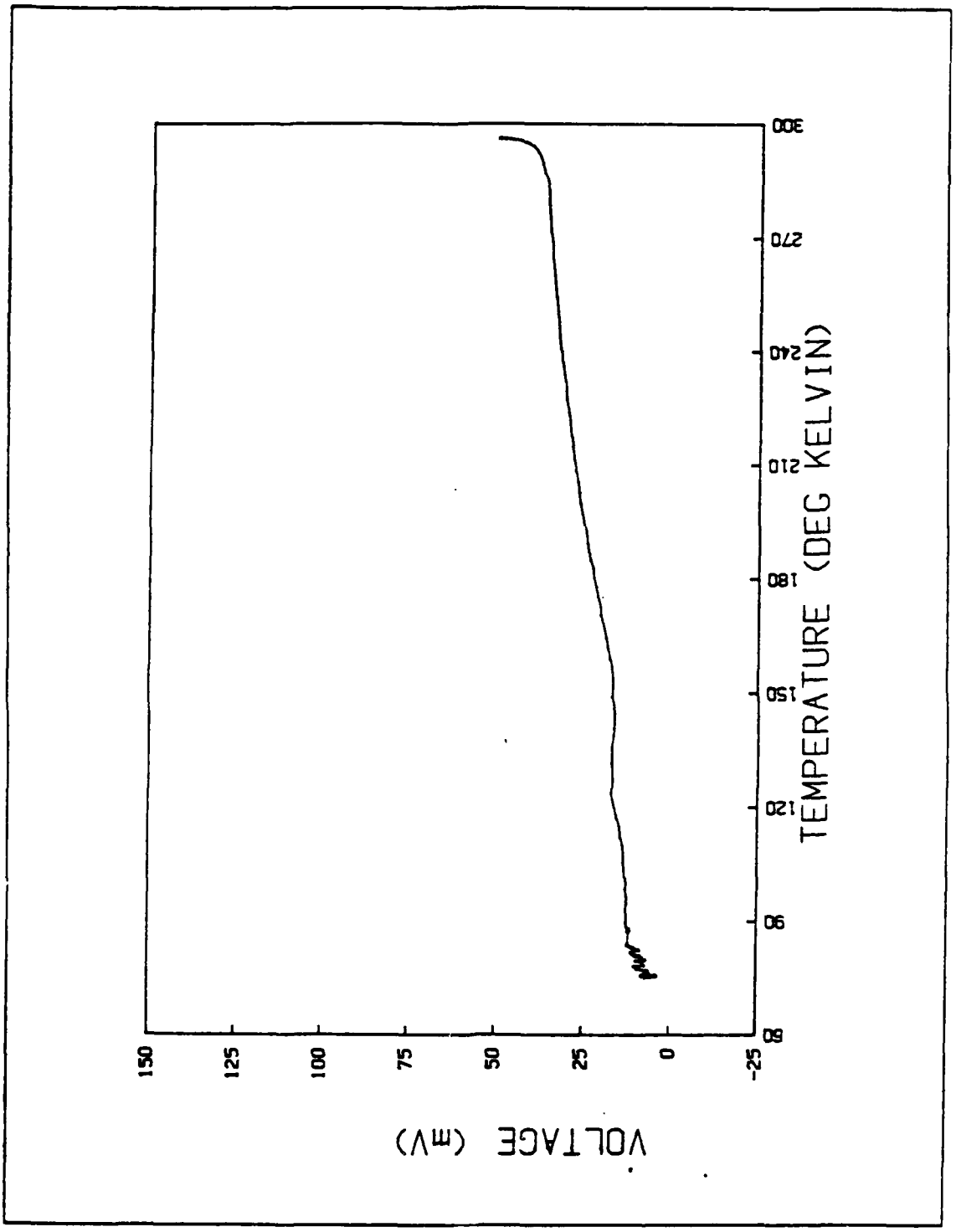

Figure 17. Sample 8 Voltage vs Temperature Curve (Post-irradiation)

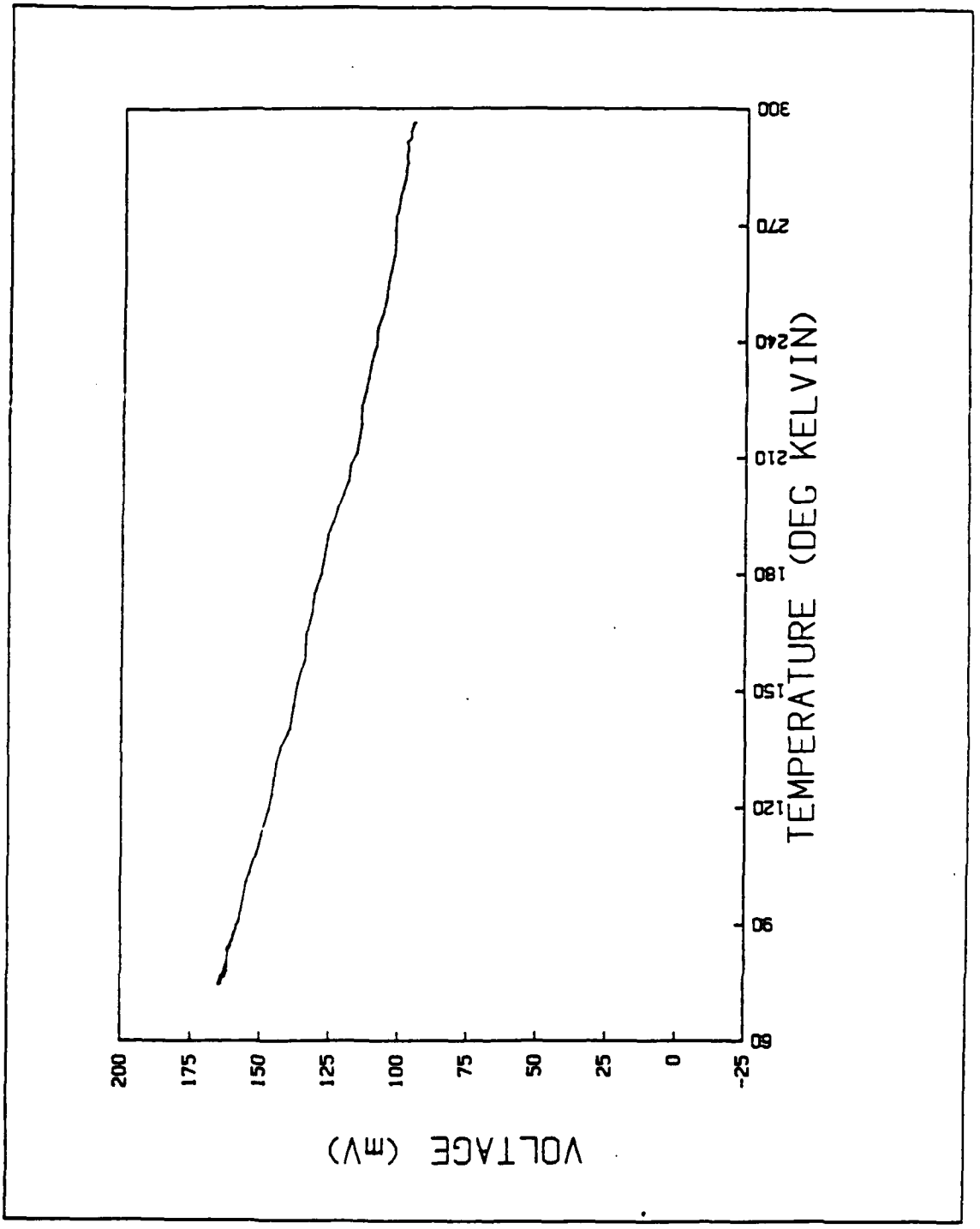

Figure 18. Sample 9 Voltage vs Temperature Curve (Post-irradiation)

Table 1. OMEGA WEST REACTOR FLUX: (Ref. 34)

Energy Range, MeV	Flux Integral (n/cm^2-s)	Error, %
Total	1.81×10^{14}	5
Thermal	7.3×10^{13}	15
>0.11	5.7×10^{13}	9
>1.0	2.9×10^{13}	7
>5.0	2.0×10^{12}	11
>10.0	4.5×10^{10}	16

Table 2. HTS PRE-IRRADIATION DATA

Sample	1	2	3	4	5	6	7	8	9
Composition[1]	b	b	a	b	a	a	b	b	a
Meissner Effect	no	no	yes	yes	yes	yes	yes	yes	yes
Size[2]	1	1	1	1	2	2	1	1	1
Lead Configuration[3]	-	-	s	s	s	s	s	s	s
Four Terminal Current (mA)	-	-	7	50	10	50	50	40	2
T_c (k)	-	-	83	88	90	87	76	88	83
Lowest Temperature (K)	-	-	70.3	70.0	70.6	70.3	70.3	70.0	70.6
Pressure (mm Hg)	-	-	304	291	316	304	304	291	316
Final Voltage Drop (mV)	-	-	0.08	0.06	0.06	0.07	0.09	0.06	0.08

Notes:
1. a = $YBa_2Cu_3O_7$ b = $ErBa_2Cu_3O_7$
2. 1 = 1.3 cm diameter. 0.5 cm thick ; 2 = 0.65 cm diameter, 0.3 cm thick
3. S = square L = linear P = around perimeter

Table 3. HTS POST-IRRADIATION DATA

Sample	4	5	6	7	8	9
Fluence[1]	a	a	b	b	c	c
Meissner Effect	d[2]	d	no	no	no	no
Lead Configuration	-	-	s	l	p	p
Four Terminal Current (mA)	-	-	.5	.5	.5	.5
T_c (K)[3]	-	-	81	n	n	n
Lowest Temperature (K)	-	-	70.2	70.2	70.7	70.2
Pressure (mm Hg)	-	-	298	298	324	298
Final Voltage Drop (mV)	-	-	0.14	0.18	3.50	164.2

Notes:
1. a = 5.2×10^{17} b = 5.2×10^{18} c = 2.2×10^{18} neutrons/cm^2
2. Destroyed and retained at Los Alamos
3. n = no transition

APPENDIX B. HTS MEASUREMENT CONTROL PROGRAM

```
1       CREATE "RESTEMPX",7,100 ! CREATES DATA FILE:REPLACE X WITH NEW FILE NAME
100     DEG ! SETS DEGREE MODE FOR AXIS LABLE ORIENTATION
200     REAL R(200),V(200),T(200) ! 1X1 DATA ARRAYS. R=SAMPLE VOLTAGE, V=THERMO-
201     ! COUPLE VOLTAGE, T= KELVIN TEMPERATURE
300     PLOTTER IS 707 ! DESIGNATES PLOTTER ADDRESS CODE
400   ! GRAPHALL ! TAKE OUT WHEN USING PLOTTER;KEEP FOR CRT
500     LOCATE 20,130,15,90 ! SETS PLOTTING BOUNDRIES
600     SCALE 60,300,-25,200 ! 1ST TWO DIGITS FOR X AXIS LIMITS, 2ND TWO FOR
601     ! Y AXIS LIMITS.
700     FXD 0 ! NUMBER OF  DECIMAL PLACES IN AXIS LABLES.
800     LAXES 30,25,60,-25 ! 1ST 2 DIGITS ARE FOR TIC MARK SPACING ON AXES;

801     ! 2ND TWO DIGITS ARE FOR COORDINATES OF ORIGIN.
900     FRAME ! PUTS A FRAME AROUND THE GRAPH
1000    MOVE 180,-40 ! MOVES THE PEN TO THE COORDINATES LISTED.
1100    LORG 4 ! CENTERS THE LABEL BELOW AT PT (180,-40)
1200    CSIZE 6 ! SIZE OF LABLE LETTERS
1300    LABEL "TEMPERATURE (DEG KELVIN)"
1400    MOVE 35,25 ! POSITIONS PEN TO Y AXIS FOR LABLING
1500    LORG 1 ! PUTS THE 'V' IN LABEL BELOW AT ( 35,25)
1600    LDIR 90 !  REORIENTS THE Y AXIS LABLE SO IT IS VERTICLE
1700    CSIZE 6 !  THIS IS THE SIZE OF THE Y AXIS LABLE LETTERS
1800    LABEL " VOLTAGE (mV)" ! Y AXIS LABLE
1900  ! END ! FALSE END FOR DEBUG
2000  ! CLEAR 722 ! THIS CMD PUTS DEVICE 722 IN ITS DEFAULT POSITION
2100    PRINTER IS 702,80 ! ADDRESS CODE OF PRINTER, # CHARACTERS PER LINE
2200    N=0 ! INITIALIZES INCREMENTAL VARIABLE N
2300    OUTPUT 722 ;"V(N)" ! ASSIGNS Nth OUTPUT OF DEVICE 722 TO ARRAY V
2400    ENTER 722 ; V(N) ! PUTS Nth ELEMENT OF ARRAY V INTO COMPUTER
2600    LET E=V(N)
2700    LET N=N+1 ! INCREMENTS COUNTING VARIABLE N , START OF COLLECTION LOOP
2800    FOR N=1 TO 199 ! SPECIFIES NUMBER OF DATA POINTS TO BE TAKEN
2900    WAIT 3000 ! TIME IN msec BETWEEN DATA POINTS
3000    OUTPUT 722 ;"V (N)" ! OUTPUT OF DEVICE 722 ASSIGNED TO ARRAY V
3100    ENTER 722 ; V(N) ! ENTERS OUTPUT OF 722 AS Nth ELEMENT OF ARRAY V
3200    ! PRINT " VOLTAGE ARE    ";V(N) ! USED FOR DEBUG
3300    IF V(N)<E THEN 3500 ELSE 2600 !  CHANGE INEQUALITY FOR UPRAMP/DOWNRAMP
3400    ! R(N)=50 ! ASSIGNS CONSTANT VALUE TO R FOR DEBUG
3500  ! CLEAR 723 !  USE OF THIS STMT SHIFTS THE METER TO DEFAULT VALUES
3600    OUTPUT 723 ;"R(N)" ! OUTPUT OF 723 ASSIGNED TO ARRAY R
3700    ENTER 723 ; R(N) ! ASSIGNS Nth ELEMENT OF R TO HP 86B COMPUTER
3701    LET V(N)=V(N)*1000 ! USED TO CHANGE TO millivolts FOR CONVERSION BELOW
3710    T(N)=-.015863+16.9113*V(N)-.262371*V(N)^2+.0672994*V(N)^3+.0138366*V(N)^4
+.00126431*V(N)^5+273 ! POLYNOMIAL CONVERTS THERMOCOUPLE mV TO KELVINS
3800    ASSIGN# 1 TO  "RESTEMP"
3900    PRINT# 1 ; T(N),R(N) ! RECALLING T AND R FOR PLOTTING
4000    ASSIGN# 1 TO  * ! CLOSES THE DATA FILE
4100    !  PRINT R(N) ! USED FOR DEUG
4200    !  PRINT V(N) ! USED FOR DEBUG
4300    PLOT T(N),R(N) ! PLOTTING COMMAND
4400    ! LABEL C
4500    NEXT N ! CONTINUES LOOP FOR N+1TH ELEMENT
4600    ASSIGN# 1 TO  "RESTEMP" ! OPENS RESTEMP FILE
4610    PRINT "                  RESISTANCE VS TEMPERATURE DATA  " ! DATA TITLE
4620    PRINT USING " 3/,3X,11A, 7X, 6A,14X,12A" ; "TEMPERATURE","SAMPLE","THERMO
COUPLE" ! NEXT TWO LINES ARE FOR DATA COLUMN HEADERS
4630    PRINT USING "3X,18X,7A,13X,7A,2/" ! "VOLTAGE","VOLTAGE"
4700    FOR N=1 TO 199
4820    PRINT T(N),R(N),V(N)
4900    NEXT N !
5000    ASSIGN# 1 TO  * ! CLOSES THE RESTEMP FILE
5100    END
```

APPENDIX C. OMEGA WEST REACTOR TEST POSITIONS

Obtained from Los Alamos National Laboratory (Ref. 34)

Facility	Location	Maximum Sample Size	Thermal-Neutron Flux at 8 MW n/cm^2-sec	Comments	
Thermal Column Rabbits				Cd Ratio (Au)	Ambient Temp.(°C at 8 MW
*TCR-1	TC-2S	9 mm dia × 57 mm	3.4×10^{12}	9.0	60.8
*TCR-2	TC-1S	"	4×10^{12}		78.1
*TCR-3	TC-3S	"	2×10^{12}		60.2
TCR-4	TC-1S	"	9.7×10^{12}	2.75	107.7
TCR-5	TC-1N	"	"	2.75	112.5
TCR-8	TC-1N	"	$\sim 5 \times 10^{12}$		
TCR-6	TC-1N	20 mm dia × 12 cm	1×10^{13}	2.7	
†TCR-7	TC-1N	(40 cc)	"	2.7	
†TCR-9	TC-1N		"	2.7	
†TCR-10	TC-1N	9 mm dia × 57 mm	6×10^{12}	4.5	
TCR-11	TC-1N	"	5×10^{12}	6.4	
Epithermal Rabbit	So. Upper Thru Port	"			
End-Port Rabbit	So. beam port, 1 in. from so. face of core	0.4 in dia by 1.9 in. long	4×10^{13}	Sample terminal is water cooled. Radiation heating is 0.5 W/g.	
Hydraulic Rabbit	Core position 3-E	0.75 in dia by 1.6 in long	9×10^{13}	Radiation heating is 5.0 W/g. Sample is water cooled.	
In-Core Samples or Experiments	Core positions 4-B, 4-D, 4-F, & 4-H	Up to 2.09 in. dia., length not restricted	6×10^{13} to 9×10^{13}	Other core positions can be used by altering core-loading pattern.	
North and South Vertical Ports	2.5 in. from NW and SW corners of core	3.5 in. dia., about 12 in. long	1.6×10^{13}	Radiation heating is 0.3 W/g. Cooling must be separately provided for samples requiring it.	
Thermal Column Ports (19)	Thermal column	Ports up to 12 × 12 in.	From 1.6×10^{9} to $\sim 5.6 \times 10^{13}$		
Upper & Lower Through Ports	Across west side of Be reflector	6 in. in dia., length not restricted	2.5×10^{12}	Ports accessible from each end.	

*Samples may be pneumatically transferred to and from CHEM ROOM.

†Dedicated to automatic Delayed Neutron and Neutron Activation Analysis Systems.

LIST OF REFERENCES

1. Edelsack, E. S., et al., "The Rocky Road to Superconductivity", Compilation of NRL Publications on High Temperature Superconductivity, Naval Research Laboratory, 1987.
2. Fishlock, D., A Guide to Superconductivity, Macdonald and Co., 1969.
3. Reitz, J. R., Milford F. J. and Christy, R. W., Foundations of Electromagnetic Theory, 3d ed., Addison-Wesley Publishing Co., 1980.
4. Parks, R. D., Superconductivity, Marcel Dekker, Inc., 1969.
5. Tinkham, M., Superconductivity, Gordon and Breach Science Publishers, Inc., 1965.
6. Khurana, A., "The T_c to Beat is 125 K", Physics Today, v. 41, April, 1988.
7. Proceedings, Naval Consortium for Superconductivity, Naval Research Laboratory, August, 1988.
8. Reed, R. P. and Clark, A. F., eds., Materials at Low Temperatures, American Society for Metals, 1983.
9. Zafiratos, C., Physics, John Wiley and Sons, Inc., 1976.
10. Bardeen, J., Cooper, L. N. and Schrieffer, J. R., Physical Review, 108, 1234, 1957.
11. MacKinnon, L., Experimental Physics at Low Temperatures, Wayne State University Press, 1966.
12. Eisberg, R. and Resnick, R., Quantum Physics of Atoms, Molecules, Solids, Nuclei and Particles, 2d ed., John Wiley and Sons, Inc., 1985.
13. Walter, U., et al., Physical Review B, 35, 5327, 1987.
14. Battlog, B., et al., Physical Review Letters, 58, 2333, 1987.
15. Bourne, L. C., Physical Review Letters, 58, 2337, 1987.
16. Weber, W., Physical Review Letters, 58, 1371, 1987.
17. Hor, P. H., et al., Physical Review Letters, 58, 1891, 1987.
18. Robinson, A. L., "More Superconductivity Questions Than Answers", Science, v. 237, p. 248, 17 July 1987.
19. Toth, L., et al., "Relationship Between Processing Procedure, Crystal Structure and Superconducting T_c in the Y-Ba-Cu-O System", Compilation of NRL Publications on High Temperature Superconductivity, Naval Research Laboratory, 1987.
20. Golben, J. P., et al., Physical Review B, 35, 8705, 1987.
21. Pauling, P., Physical Review Letters, 35, 1234, 1987.

22. Thomsen, D. E., "Superconductivity and Quantum Mechanics", Science News, v. 131, June, 1987.

23. Sanchez, R., et al., Physical Review B, 37, 3678, 1988.

24. Olesen, H. L., Radiation Effects on Electronic Systems, Plenum Press, 1966.

25. Harwood, J. J., et al., eds., The Effect of Radiation on Materials, Reinhold Publishing Co., 1958.

26. Glasstone, S., and Dolan, P. J., The Effects of Nuclear Weapons, 3d ed., Department of Defense, 1977.

27. Kircher, J. F., and Bowman, R. E., eds., Effects of Radiation on Materials and Composites, Reinhold Publishing Co., 1964.

28. Maisch, W. G., et al., IEEE Transactions on Nuclear Science, December, 1987.

29. Bretherick, L., ed., Hazards in the Chemical Laboratory, The Royal Society of Chemistry, 1986.

30. Toth, L., et al., "Processing of High T_c Superconductors: Structure and Properties", Compilation of NRL Publications on High Temperature Superconductivity, Naval Research Laboratory, 1987.

31. HP 3456A Digital Multimeter Technical Manual, Hewlett Packard Corporation, 1985.

32. Omega Complete Temperature Measurement Handbook and Encyclopedia, Omega Engineering, Inc., 1987.

33. White, G. K., Experimental Techniques in Low Temperature Physics, Oxford at the Clarendon Press, 1968.

34. Omega West Reactor Specification Sheet, Los Alamos National Laboratory, 1987.

35. Hyde, J., "High Temperature Superconductivity" Nature, v. 327, p. 403, 4 June 1987.

36. Sweigard, E. L., Effects of 63.5 MeV Electron Irradiation on Y-Ba-Cu-O and Gd-Ba-Cu-O High Temperature Superconductors, Master's Thesis, Naval Postgraduate School, Monterey, CA, December, 1987.

37. Willis, J., et al., Radiation Damage in $YBa_2Cu_3O_7$ by Fast Neutrons, Los Alamos National Laboratory, 1988.

38. Atobe, N., Physical Review B, 36, 7194, 1987.

39. Dienes, G. J. and Vineyard, G. H., Radiation Effects in Solids, Volume I, Interscience Publishers, Inc., 1957.

INITIAL DISTRIBUTION LIST

		No. Copies
1.	Defense Technical Information Center Cameron Station Alexandria, VA 22304-6145	2
2.	Library, Code 0142 Naval Postgraduate School Monterey, CA 93943-5002	2
3.	Professor X. K. Maruyama, Code 61 Mp Department of Physics Naval Postgraduate School Monterey, CA 93943-5000	4
4.	Professor F. R. Buskirk, Code 61 Bs Department of Physics Naval Postgraduate School Monterey, CA 93943-5000	4
5.	Professor K. E. Woehler, Code 61 Wo Department of Physics Naval Postgraduate School Monterey, CA 93943-5000	2
6.	LCDR J. J. Hammerer USS Halyburton (FFG-40) FPO MIAMI 34091-1495	2
7.	Los Alamos National Laboratory ATTN: Dr. R. D. Brown Mail Stop H840 P.O. Box 1663 Los Alamos, NM 87545	1
8.	Naval Research Laboratory ATTN: Dr. S. A. Wolf Washington, DC 20375	1
9.	Naval Research Laboratory ATTN: Dr. M. S. Osofsky Washington, DC 20375	1
10.	Office of Naval Research ATTN: Dr. Richard Brandt 1030 East Green Street Pasadena, CA 91106	1

11. Office of Naval Technology
ATTN: Dr. Frank Menotti
800 N. Quincy Street
Arlington, VA 22217 — 1

12. Office of Naval Technology
ATTN: Mr. James Cauffman
800 N. Quincy Street
Arlington, VA 22217 — 1

13. Dr. D. Ederer
National Bureau of Standards
Bldg. 221, Rm.A251
Gaithersburg, MD 20899 — 1

14. Chief of Naval Operations
OP-322C
Washington DC 20350-2000 — 1

15. Dr. J. H. Kinney
Lawrence Livermore National Laboratory
P.O. Box 808
Livermore, CA 94550 — 1

16. L. J. Dries, Code 9740-202
Research and Development Division
Lockheed Missiles and Space Company, Inc.
3251 Hanover Street
Palo Alto, CA 94304-1191 — 1

17. Los Alamos National Laboratory
ATTN: Dr. M. Bunker
Mail Stop G776
P.O. Box 1663
Los Alamos, NM 87545 — 1

18. Dr. T. Hofler, Code 61 Hf
Department of Physics
Naval Postgraduate School
Monterey, CA 93943-5000 — 1

19. Mr. G. Pless, Code 61
Department of Physics
Naval Postgraduate School
Monterey, CA 93943-5000 — 1